# Ontogenetic development of the holocephalan dentition: Morphological transitions of dentine in the absence of teeth

Zerina Johanson[1], Esther Manzanares[2], Charlie Underwood[1, 3], Brett Clark[4], Vincent Fernandez[4], Moya Smith[1, 5]

[1]Department of Earth Sciences, Natural History Museum London, UK
[2]Institut Cavanilles de Biodiversitat i Biologia Evolutiva, Universitat de Valencia, Paterna, 46980, Valencia, Spain
[3]Department of Earth and Planetary Sciences, Birkbeck, University of London, London, UK
[4]Core Research Laboratories, Natural History Museum, London, UK
[5]Centre for Craniofacial and Regenerative Biology, King's College London, UK

**Abstract**

Among the cartilaginous fishes (Chondrichthyes), the Holocephali are unique in that teeth are absent both in ontogeny and adult regenerative growth. Instead, the holocephalan dentition of ~~statodont~~ ever-growing non-shedding dental plates is composed of dentine, trabecular in arrangement, forming spaces into which a novel hypermineralized dentine (whitlockin) is deposited. These tissue features form a variety of specific morphologies as the defining characters of dental plates in the three families of extant holocephalans. We demonstrate how this morphology changes through ontogenetic development with continuity between morphologies, through successive growth stages of the ~~statodont~~ dentition represented by the dental plate. For example, rod-shaped whitlockin appears early, later transformed into the tritoral pad, including a regular arrangement of vascular canals and whitlockin forming with increasing mineralization (95–~~–~~98%). While the tritoral pads develop lingually, stacks of individual ovoids of whitlockin replace the rods in the more labial parts of the plate, again shaped by the forming trabecular dentine. The ability to make dentine into new, distinctive patterns is retained in the evolution of the Holocephali, despite the lack of teeth forming in development of the dentition. We propose that developmentally, odontogenic stem cells, retained through evolution, control the trabecular

dentine formation within the dental plate, and transition to form whitlockin, throughout life-time growth. Our model of cellular activity proposes a tight membrane of odontoblasts, having transformed to whitloblasts, that can control active influx of minerals to the rapidly mineralizing dentine, forming whitlockin. After the reduced whitloblast cells transition back to odontoblasts, they continue to monitor the levels of minerals (calcium, phosphate, magnesium), and at a slower rate of growth in the peritubate 'softer' dentine. This model explains the unique features of transitions within the holocephalan dental plate morphology.

**KEYWORDS**

Holocephali, dentition, dentine, whitlockin, odontoblasts, Chondrichthyes

## INTRODUCTION

Holocephali, the sister group of Elasmobranchii (sharks, rays), is perhaps the most enigmatic and least understood group of Chondrichthyes. The small numbers of holocephalan species living today are primarily deep-water fishes (Callorhinchidae, Chimaeridae, Rhinochimaeridae; Fig. 1), although the Family Callorhinchidae inhabits shallow coastal environments (Didier, 2004). Holocephalans are characterized by the fusion of the upper jaw to the cranium and the presence of ever-growing dental plates (Patterson, 1965, 1992; Didier, 1995; Lund & Grogan, 1997; Stahl, 1999; Smith et al., 2019). Their dentition is composed of six dental plates, four in the upper jaw and two in the lower, representing a unique system that is made entirely of dentine, supported by the poorly mineralized (tessellated) cartilage of the jaws. These dental plates possess some of the most hypermineralized tissues in holocephalans, and have been the focus of much of the research on this group, including a rich fossil record (Schauinsland, 1903; Dean, 1906, 1909; Moy-Thomas, 1936, 1939; Patterson, 1965, 1992; Ørvig, 1967, 1985; Lund, 1977, 1986, 1988; Zangerl, 1981; Ishyama & Sasagawa, 1984; Ishyama et al., 1991; Kemp, 1984; Zangerl et al., 1993; Didier et al., 1994; Didier, 1995, 2004; Duffin & Delsate, 1995; Stahl, 1999; Popov 2003; Smith et al., 2019, 2020; Johanson et al., 2020).

The entire feeding system in extant holocephalans develops in ontogeny and growth without forming separate teeth, instead utilizing the redeployment of a very specialized, high-mineral content dentine into different morphologies, which is a feature of their

diversity and evolution (Johanson et al., 2020). The dental plates are morphologically distinct at the surface in adults and form the basis for taxonomic identification of different species (e.g., Patterson, 1965; Stahl, 1999). The entire plate tissue is composed of dentine, including a two-layer outer shell of the plate (Smith et al., 2019). The subsequent infilling of hypermineralized dentine into spaces formed within the trabecular dentine produces the functionally resistant tissue at the worn surface (Kemp, 1984; Ørvig, 1985; Didier, 1995; Stahl, 1999; Smith et al., 2019).

In this paper we concentrate on how dental morphologies are achieved in ontogeny, in particular the relationships between the hypermineralized structures known as rods, ovoids and tritoral pads. Each dental plate continues to grow throughout the adult phase as a type of replacement growth found in ~~all statodont~~ever-growing dentitions (retention of dental material, rather than shedding), including growth of new morphologies of the hypermineralized dentine. Individual teeth have been lost in evolution (Moy-Thomas, 1936; Patterson, 1965; Lund, 1977; Didier, 1995; Stahl, 1999; Johanson et al., 2020), and dental plates lack enamel, or enameloid, a co-operatively formed hard tissue between epithelium (ameloblasts) and ectomesenchyme (odontoblasts). As an alternative solution, the hypermineralized dentine, a unique tissue type from its crystal identity (Ishyama & Sasagawa, 1984; Smith et al., 2019; Iijama & Ishyama, 2020), provides different degrees of hardness throughout the dental plate. All dentine is derived from embryonic cranial ectomesenchyme (Miletich & Sharpe, 2004), including in fishes (Kundrát et al., 2008), so this holocephalan specialization is part of the repertoire of these cells determining all tissue morphologies. We have previously suggested that the pattern of hypermineralized dentine deposition in renewal growth begins in association with multiple distinct ridges formed by the developing, lingual outer dentine surface of the dental plate (Smith et al., 2020). Here, the contact between stem odontogenic neural crest cells in pulpal tissue and epithelium of the dental lamina can regulate position, timing and growth of the specialized hypermineralized dentine. As well, this dentine differs in mineral composition, being very high in magnesium (Mg), closest to the mineral whitlockite (Ishyama & Sasagawa, 1984; Iijima & Ishiyama, 2020). We termed this dentine ‘whitlockin’, with a much lower percentage of hydroxyapatite compared to the less highly mineralized framework trabecular dentine (Smith et al., 2019).

We propose to ~~clarify the histologies of~~investigate the types of dentine within a developmental concept of one cell type, namely the odontoblast, identified from the cell spaces of tubules and lacunae, as visualised in both ground sections and virtual sections from CT-scanning. ~~which~~ This cell type makes all components of the holocephalan dentition and we propose two scenarios, that either odontoblasts transform into whitloblasts, or, they are replaced from stem cells as novel cells to make this hypermineralized dentine. In extant holocephalans this occurs in the developmental absence of teeth, and axiomatically without osteoblasts, in the absence of bone.

**Materials and Methods**

Specimens used in this study were obtained from a number of sources. The majority of the European specimens were obtained from trawls by the Marine Scotland research vessel MRV Scotia in 2015 and 2017, arriving on deck already dead. These, including *Chimaera monstrosa* Linnaeus, 1758 and *Hydrolagus pallidus* Hardy & Stehmann, 1990, were dissected and/or defleshed at Birkbeck College, London and transferred to the Natural History Museum (NHM). An additional specimen of a juvenile *Hydrolagus affinis* (de Brito Capello, 1868) was already present within the NHM Life Sciences fish collection. Some specimens (obtained as dried whole or defleshed material) were obtained from commercial sources in Uruguay (*Callorhinchus callorhinchus* Linnaeus, 1758), Taiwan (*Chimaera* sp.) and the Philippines (Chimaeridae indet.). An embryo of *Callorhinchus milii* Bory de Saint-Vincent, 1823 was provided by Dr. Catherine Boisvert (Curtin University, Perth), from Monash University, Victoria, Australia (see Johanson et al. 2015 for further details regarding this specimen). No surgical procedures or experiments were performed on the specimens described herein.

Specimens were CT-scanned in the Image and Analysis Centre, NHM, using a Nikon HMXST 225. A filtered back projection algorithm was used in reconstructing the projections, using the CT-agent software (Nikon Metrology GmbH, Alzenau, Germany), producing a 16-bit uncompressed raw volume. Other specimens were CT-scanned at Kings College London using a Scanco µCT50 microCT scanner (Scanco, Brüttisellen, Switzerland). The specimens were characterized using the density profile tool of the Parallax Microview software package (Parallax Innovations Inc., Ilderton, Canada), after

downsampling to 24 μm voxel size. CT-scanning parameters are listed in Supplementary Information Table 1. μCT data were 3D rendered using Avizo software (https://www.fei.com/software/amira-avizo/) and rotatable 3D mesh model .stl files produced (NHM Data Portal: data.nhm.ac.uk/dataset/ontogenetic-development-of-the-holocephalan-dentition). Institutional abbreviations: BMNH, Life Sciences, Natural History Museum, London; NHMUK PV P, Earth Sciences fossil fish collections, Natural History Museum, London.

**Developmental Observations**

The specialized hypermineralized whitlockin is deposited within preformed spaces in the trabecular dentine and first develops as a tissue with little mineralization (Smith et al., 2019, and see Discussion). The preformed spaces take a variety of shapes, including elongate rods, separate rounded ovoids, or extensive tritoral pads. In the latter, regularly spaced vascular canals run through the tissue, narrowed by infilling with less mineralized, peritubate dentine; wear of this mineralized dentine creates the characteristic punctate hard tissue at the oral surface (Didier, 1995; Stahl, 1999; Smith et al., 2019). But, as Didier (1995; also Garman, 1904) previously noted, there is a developmental continuity between rods, ovoids, and pads that blurs the distinction between these.

We have observed that the tritoral pads of *Chimaera* develop from rods (Smith et al., 2020) but here expand upon this description through earlier growth stages of both *Chimaera* and *Hydrolagus* (Family Chimaeridae), with tritoral pads and ovoid series being present in later stages. Of the extant holocephalans, early growth stages of *Callorhinchus* dental plates (Family Callorhinchidae) have been the most often described (Schauinsland, 1903: figs. XX, XXI; Garman, 1904: pl. 6.3, 6.4; Didier et al., 1994; Kemp, 1984). In the Callorhinchidae, the rod-like structures are characteristic of early plate development but tritoral pads alone are present at later stages. In both families, earlier stages of development are characterized by the outer dentine layers and an internal trabecular dentine framework alone; notably, elongate folds are present on the oral surface of the outer dental layer, within which the early pattern of dentine, the rods, is formed.

**Family Callorhinchidae: *Callorhinchus milii, Callorhinchus callorhinchus***

*Callorhinchus milii*

At the earliest growth stage available, a late stage embryo, the upper dentition includes a small, rounded anterior dental plate and a substantially larger posterior plate (ADP, PDP; Fig. 2A–C). On the oral face of the posterior plate, are two antero-posteriorly oriented, low and elongate folds in the plate surface, with the medial fold being longer, and the more lateral, shorter (Fig. 2A, fo). In virtual section (Fig. 2D), the elevated folds are open internally, with less mineralized dentine present within (white arrow, the dentine is darker than the surrounding trabecular dentine in this CT-scan, which indicates less mineralization). On the opposing visceral face, the posterior plate has a distinct, smooth lamina around all margins except the posterior (Fig. 2C, black arrowheads; 'descending lamina', Patterson, 1992), being best developed and widest anteriorly. More posteriorly, the developing trabecular dentine can be seen. The distinct ridge and developing trabecular dentine can also be seen on the smaller anterior plates (Fig. 2C, small white arrow, trab). Along the anterolateral margin of the posterior dental plate are a series of large, closely spaced openings into the plate (Fig. 2B, black arrowheads).

On the lower dental plate, a single wider, more sinuous fold is present on the oral face. Compared to the folds on the upper posterior plate, this fold is clearly open posteriorly, such that the forming dentine enclosed within is visible (Fig. 2E, white arrowheads). This developing dentine can also be seen in section (Fig. 2F, white arrows). The lateral openings along the upper posterior dental plate are not visible on the lower plate, although this margin is open such that the trabecular dentine is visible (Fig. 2E). On the visceral surface, the lamina seen on the posterior upper plate is absent, but there is a smooth face anteriorly (Fig. 2G, asterisk). More posteriorly, developing trabecular dentine is visible; on all plates, this represents the surface where active growth occurs.

In the next available growth stage, representing a terminal stage embryo or hatchling neonate (Fig. 2H–L), the plates are better developed, particularly the anterior upper dental plate, which is triangular in shape, with a curved fold crossing its surface (Fig. 2I). The early development of the hypermineralized dentine can also be visualized (white density value associated with the fold indicating increased mineralization). This is also the case with the two folds on the upper posterior plate, with mineralized dentine most apparent in the middle of the elevated folds (Fig. 2I, black arrowheads). On the visceral surface of both

upper dental plates, the descending lamina is well developed (Fig. 2J, black arrowheads). Compared to the earlier growth stage, the trabecular tissue surrounded by this lamina appears to be predominant and separated from the descending lamina by a groove on the posterior dental plate. The corresponding surface of the anterior dental plate is complex, with a short lamina along the lateral margins present (Fig. 2J, white arrowhead), with the more medial, antero-posteriorly oriented descending lamina defining the area of trabecular dentine deposition (Fig. 2J, black arrowheads).

On the oral surface of lower dental plates, two folds are present posteriorly, that converge anteriorly to form a lateral marginal fold (Fig. 2K, white arrowhead). The medial fold is wider than the more lateral fold, and in both, the hypermineralized dentine deposited inside is concentrated in the middle part of the plate (Fig. 2K, red, L, virtually dissected). At this growth stage, distinct curved margins indicate that this dentine is developing around blood vessels, in some instances completing their enclosure (Fig. 2L, white arrows, white arrowhead).

In the latest growth stage available for *Callorhinchus milii* (Fig. 2M–O), the lower dental plate shows a single, well-developed tritoral pad formed of mineralized dentine, with a punctate surface representing the openings to the vascular canals, closed by deposition of peritubate dentine (Fig. 2M, O, tri, vasc). The tritoral pad bifurcates anteriorly; there are no other mineralized elements associated with the dental plate. On the opposing face (Fig. 2N, white arrowheads), the descending lamina is large, widest anteriorly. Trabecular dentine is developing within the anterior part of this lamina, which can also be seen in section view (Fig. 2O, trab). The tritoral pad and lamina represent the oral and aboral territories described by Didier et al. (1994; oral, abor), separated at the point indicated by the white arrow. These three individuals of *Callorhinchus milii* demonstrate growth as a developmental timed series, with folds in the earlier stages marking the location of initial deposition of mineralized dentine through to what will become the highly mineralized territories of the tritoral pads.

*Callorhinchus callorhinchus*

Given differences in mineralization, t~~Two T~~he individual in Figure 3A–G is considered to be younger and in Figure 3H–M,~~of the two, both represent~~ing ~~different sized individuals.~~

the older ~~in (Fig. 3H, I~~3. These show different dental plate morphologies, particularly with respect to the distribution of whitlockin within them (Fig. 3A, B, D, E, H, I, K, L). In the ~~first~~ younger individual (Figure 3A–G), ~~this~~ the hypermineralized dentine is present as two elongate tritoral pads in the posterior upper dental plate (Fig. 3A, B). In the lower dental plate, one main tritor pad is present along with a narrower pad laterally (Fig. 3D, E) with a region without vascularized whitlockin at the anterior margin of the dental plate. In section (Fig. 3C, F, G), the tritoral pads are supported by the trabecular dentine forming the main part of the dental plate.

However, in the second individual a different morphology is apparent, as only a single tritoral pad is present in the upper posterior dental plate (Fig. 3H, I), with a bilobed anterior margin and a single pad dominates the lower dental plate as well. ~~The individual in Figure 3A–G is considered to be younger, as in~~In the tritoral pads (Fig. 3A–G), the vascular canals are wider (more open) compared to the individual in Figure 3H–M, indicating less dentine deposition within the canals, and overall less mineralization. As well, in section, the tritoral pad dentine in the younger individual (Fig. 3F, G) is less mineralized (darker tone) compared to that in the older individual (Fig. 3J, M, brighter tone).

**Family Chimaeridae**: ***Hydrolagus affinis*, *Hydrolagus pallidus***
***Chimaera monstrosa, Chimaera* sp. and Chimaeridae indet.**

*Hydrolagus affinis*

Three specimens from earlier developmental stages were available, one with a dentition comprising primarily the framework of the outer dentine layer (Fig. 4A–I), and the others from later stages with more highly mineralized dentine present (Fig. 5). In the first individual (Fig. 4A, B), all three pairs of dental plates are present, with smaller, triangular anterior upper dental plates, and larger, cleaver-shaped posterior dental plates (Fig. 4C, plates false coloured green [lower]; red [anterior upper], blue [posterior upper dental plates). The lower jaw dental plates are rectangular in shape (Fig. 4C, G). The visceral margins of the dental plates are open, and the plates appear largely empty internally, at least close to the edge (Fig. 4D, op). Large pores are present on the plates of the upper dentition. On the anterior plate there are two pores positioned posterolaterally, while on the posterior plate there is a larger opening in the anteromedial part of the plate, and other pores along

the posterior plate margin (Fig. 4C–F, po). The anteromedial pore appears to be related to the fold and internal rod on the posterior dental plate, all being parasymphysial in position (compare Fig. 4C, E, F). However, the more posterolateral pores on the posterior plate do not seem to be related to a fold at this growth stage. On the lower dental plate, pores are less clearly present, but two folds are apparent, one parasymphysial, and the second more lateral in position (Fig. 4C, G, I, p.fo). The more lateral fold is better developed, and in virtual section the open spaces under these folds are visible (Fig. 4H, fo.op, p.fo.op), and developing rods can be seen within (e.g., Fig. 4I, rd, parasymphysially). Virtual dissections of these rods are available on the NHM Data Portal (data.nhm.ac.uk/dataset/ontogenetic-development-of-the-holocephalan-dentition).

By comparison, in the representatives of the next growth stages (Fig. 5), hypermineralized dentine is evident within all plates, including elongate rods, ovoid series and patches of irregular mineralization, all extending along the labial plate margin (Fig. 5B, C, F–H, J, ov, p.rd, rd, ptch). The parasymphysial rods on the posterior upper, and lower dental plates from the previous growth stage (Fig. 4) are now better developed (Fig. 5F, H, J). The anterior upper plate is dominated by series of ovoids along the labial margin of the plate; the ovoids are defined, although not always clearly separated (Fig. 5B, C, F, G, ov). A pair of thin rods is also present parasymphysially (Fig. 5F, G, p.rd). The openings visible on the plate margins of the younger individual (Fig. 4) are no longer visible. On the posterior dental plate, thinner, less developed rods are present lateral to parasymphysial rods (Fig. 5F, H), along with a faintly developed patch of mineralization. Mineralization is better developed in the lower jaw (Fig. 5I, J), with parasymphysial rods that have irregular margins, approaching a beaded appearance, followed more laterally by a large patch of irregular mineralization and a number of rods of variable length and mineralization (Fig. 5B, J). The first of these rods just posterolateral to the irregular mineralization is the better developed (Fig. 5J, rd/tri), and the position of this rod, and the parasymphyseal rod (Fig. 5J, white asterisks) matches the position of the ridges on the lower dental plate in the earlier development stage shown in Figure 4C, G, I.

*Hydrolagus pallidus*

A single specimen of a large individual of this species is compared to the earlier ontogenetic stages of *H. affinis* (Fig. 6A–K). In the anterior upper dental plates, the ovoids are better defined, with more clearly distinct ovoids within the series (Fig. 6D, E). In place of the thin parasymphysial rods from previous growth stages are a pair of small ovoid series, much shorter than those more laterally (Fig. 6D, E, white arrows). In the posterior upper dental plates, the main parasymphysial rods appear largely unchanged, although a second pair of small, thin rods is present medial to the main pair (Fig. 6D, F, white arrowheads). The rod that was just lateral to the main parasymphysial rod in the previous growth stage has been replaced by an ovoid series and more lateral to this, elements in the region of irregular patches of mineralization have become more distinct, but are still irregular (Fig. 6F). Continuing laterally along the plate margin are irregular series of ovoids (Fig. 6F). In virtual sections, a distinct aboral territory can be seen on the posterior dental plate (Fig. 6G–I, white arrows), filled with trabecular dentine, as described in *Callorhinchus*. On the lower dental plates (Fig. 6J, K), the parasymphyseal rods have been replaced by a well-defined ovoid series, and there is now a larger ovoid series positioned on the lateral margin of the patch of irregular mineralization (Fig. 6K, white arrows). Several ovoid series follow laterally, with the most lateral being the least well-developed (Fig. 6K). More medially, there is a new irregularly mineralized rod, with a surface that appears cut by deep grooves (Fig. 6K, rd/tri).

*Chimaeridae (*Hydrolagus *or* Chimaera*) indet.*

This skull, purchased from the Philippines and presumably originating from there, is not identifiable due to the lack of detailed species-level description of extant chimaeroid dentitions. In this specimen (Fig. 6L–S), the ovoid series are well developed on the anterior upper dental plate, with the smaller and shorter parasymphseal series from the previous stage being longer (Fig. 6O, arrows). Tritoral pads are present in both the upper posterior and lower dental plates (Fig. 6N–S, tri); on the latter, there is a single broad tritoral pad (Fig. 6S). On the former, two tritoral pads are present, including an elongate pad medially and a broader one laterally (Fig. 6O–Q). These all have the typical tritoral pad morphology with small openings on the oral surface, marking the position of vascular canals running through the pad. On the posterior upper dental plate, just anterior to the elongate tritoral

pad, is a second elongate rod-like element of mineralized dentine, but the number of openings on the oral surface is much less than the tritoral pads (Fig. 6O, P, white arrowheads). On the opposing surface (Fig. 6Q, arrowhead), the surface of this rod-like element is crossed by grooves and what appear to be elongate pits; the comparable surfaces of the tritoral pads are also visible in this view, with rounded vascular canal openings clearly present. The tritoral pad elements form a medial unit on the upper posterior dental plate, while the ovoid series and the patch of irregular mineralization are positioned laterally, also present on the lower dental plate (Fig. 6S). However, on the lower dental plate, the more posterolateral series of ovoids is well separated from the patch of irregular mineralization, compared to the upper dental plate. Additionally in this specimen, there appears to be a break within the irregular mineralization and parasymphyseal ovoid series, on the left dental plate (Fig. 6S, asterisk). This is not due to damage, as no breakage is visible externally (Fig. 6R).

*Chimaera monstrosa*

Three growth stages are available for examination (Fig. 7); in the first, representing the youngest individual (Fig. 7A–H), the mineralized units in the upper dental plates are represented by a series of short rods in the anterior plate (Fig. 7D, F), while in the posterior plate, a parasymphyseal rod is present, along with two small rod-like elements posterolaterally (Fig. 7D, E, p.rd, rd). Along the lateral margin of the posterior dental plate is the patch of irregular mineralization (Fig. 7D, E, ptch) On the lower dental plate, a parasymphyseal rod is flanked by the irregular mineralization, and separated by a gap from a second rod and patch of mineralization more posterolaterally. Medial to this is a single elongate rod (Fig. 7H, ptch, rd).

In the next growth stage (Fig. 7I–O), the mineralized rods in the anterior upper dental plate are longer than in the previous growth stage (Fig. 7J, K), and a single thin rod is present parasymphyseally (Fig. 7K). In the posterior upper dental plate, in oral view, the elongate parasymphyseal rods present a smooth external surface and appear to have small dentine units being added to them (Fig. 7J, L, M, arrowheads). Figure 7M shows the opposing surface of the posterior dental plate (reversed with respect to Fig. 7L), where these new units are clearer; on both surfaces, the parasymphyseal rod shows rounded

openings developing within the rod (Fig. 7L, M, white arrows). With respect to the rod-like elements posterolateral to the parasymphyseal rods (Fig. 7D, rd), the more posterior has become noticeably elongated, while the more anterior remains short (Fig. 7L, M, asterisks). A series of rods of varying degrees of mineralization run along the lateral margin of the plate, with some small patches of irregular mineralization (Fig. 7L). In the lower dental plate, the parasymphyseal rods have elongated and the patch of irregular mineralization has increased in size and complexity (Fig. 7N, O). The more posterior rods, formed by two small elements in the previous growth stage (Fig. 7H, rd), have elongated as well, while the lateral margin of the dental plate has become more dominated by elongate and sometimes incomplete, rods (Fig. 7O).

The next stage (Fig. 7P–T), sees the replacement of the rods with ovoid series in the upper anterior dental plate, while the thinner pair of rods situated parasymphyseally remain rod-like (Fig. 7R, S, arrows). One of the ovoid series appears to have split (Fig. 7S, asterisk). In the posterior upper plate, in oral view, two rods are present (parasymphyseal and a second more posterolaterally positioned, 7R, T, p.rd, rd), with a third pair of irregular rods developing even more parasymphysially (Fig. 7R, arrowhead). With respect to the more posterolateral rods, there appears to be new mineralized dentine elements being deposited lateral to these (Fig. 7R, white arrows). This can also be seen on the opposing surface of these mineralized elements (Fig. 7T, reversed relative to Fig. 7R), where the surface of the two main rods shows developing openings (Fig. 7T, white arrows). Laterally, the number of rods has increased, these having irregular margins along their length. A small area of irregular mineralization may be present most posterolaterally.

*Chimaera* sp.

This small dried specimen from Taiwan is too distorted to identify to species level. Despite its small size (30cm total length) the dentition appears more robust (Fig. 8) than in *Chimaera monstrosa* (Fig. 7). The anterior dental plate contains multiple series of ovoids, interspersed with developing rods (Fig. 8D, ov, rd). The posterior plate is dominated by the irregular mineralization laterally (Fig. 8F, ptch) and a pair of rods/tritoral pads medially (Fig. 8F, p.rd/tri, rd/tri). Both of these rods show large openings posteriorly, with smaller and more irregularly placed openings anteriorly, although the anteriormost part of the rods

lack any openings (Fig. 8E, white arrows). In the lower dental plate, a parasymphyseal ovoid series is present flanked by a patch of irregular mineralization (Fig. 8G, p.ov, ptch). An elongate tritoral pad with characteristic vascular canal openings lies posterolaterally, with multiple thin rods at the lateral margin of the plate (Fig. 8G, tri, rd). The position of parasymphysial ovoid series and the tritoral pad can also be seen beneath the unworn surface of the dental plate (Fig. 8E).

## DISCUSSION

### Developmental Interpretations

*Importance of outer shell dentine in ~~originating~~ facilitating whitlockin deposition*

Among crown group holocephalans (Callorhinchidae, Chimaeridae, Rhinochimaeridae; Fig. 1), the upper and lower dental plates are made entirely of dentine, comprising a framework of trabecular dentine within the outer shell of dentine ~~layer~~. Also in adult plates the labial margin of this outer dentine makes a raised edge around the plate due to a higher level of mineralization. Within this structured framework, secreted by surface odontoblasts, but also with cell bodies retained within the dentine, a very high density ~~mineralized~~ dentine, whitlockin, is deposited by specialized ~~odontoblasts~~ cells referred to as whitloblasts. These whitloblasts remain on the active surface, joined as a cell layer ~~within the forming and completed tissue~~ and generating massive numbers of tubules within the whitlockin (Fig. 9E, F; Smith et al., 2019). The differing morphologies formed by the whitlockin include the simple rods of varying lengths and thicknesses, along with the tritoral pads with a punctate surface, and series of separate, rounded elements known as ‘pearl strings’ or ‘ovoid stacks’ (summarized in Didier, 1995; Stahl, 1999). As well, patches of irregular mineralization occur, differing from these three morphologies. ~~These~~ All whitlockin structures ~~all~~ have a vascular system surrounding them often close to the formative layer of cells (Smith et al. 2019: fig. 4). ~~within the trabecular dentine~~

~~However~~Importantly, the dental plates in the earliest growth stages are composed of the outer dentine layer (shell) and trabecular dentine alone (Didier et al., 1994; Didier, 1995), as for example, in *Hydrolagus* (Fig. 4C). These show folds in the outer dentine ~~layer~~ shell forming elevations crossing the oral surface of the upper and lower dental plates, combined with large pores at the margins that mark where blood vessels enter the dental

plate; these vessels could also enter the plate via the open visceral margins (e.g., Fig. 4D–F). Mineralized dentine ~~is being deposited~~forms within these folds (e.g., Fig. 4E, F, I). Comparably oriented mineralized elevations form on early dental plates of *Callorhinchus* (Garman, 1904; Fig. 2A, E, I, K, L), also with developing hypermineralized dentine visible within (Fig. 2D–F). ~~We p~~Previously, we demonstrated ~~the presence of~~ distinct sequential, spatio-temporal ridges medially (lingually) formed in the outer dentine, at the ~~formative~~ deepest growth surface of the adult dental plate (e.g., Fig. 8D, anterior dental plate, ADP). These coincided with locations of the whitlockin where it was sequestered within the trabecular spaces, as part of the ever-growing ~~statodont~~ process of dental plates ~~growth~~ (Smith et al., 2020). We suggest that these ridges, forming at the developing edge of tissue renewal in adult dentitions, and associated with epithelial tissue (Supplemental Information Fig. 1), are developmentally linked to the folded elevations seen in the embryonic growth stages of the dental plate.

*Comparative early development of whitlockin structures*

The adult dental plates of the extant Callorhinchidae are morphologically simple compared to the Chimaeridae (*Hydrolagus*, *Chimaera*) and Rhinochimaeridae (*Harriotta*, Smith et al. 2019), having only tritoral pads in both upper and lower dental plates. As noted, the tritoral pad tissues develop in the location corresponding to the elevated folds of the outer dentine shell of the oral surfaces, which traverse the plates in earlier growth stages. Small rods of dentine appear to be developing within these folds (Fig. 2D, F), while in later, but still early stages, the presence of open, curved edges (e.g., Fig. 2L) indicates that the dentine is growing to surround blood vessels medially, until the larger tritoral pad is formed. This positional relationship between the outer dentine folds and blood vessels suggests that the tritoral pad develops from an interaction between them, as supported by observations in the Chimaeridae.

In early growth stages of the dentitions in *Chimaera* and *Hydrolagus*, the dentine rods are present in all dental plates (Figs. 4, 5, 7). In one of the earliest stages available, the rods are ~~again~~ shown to develop~~ing~~ within two elevated folds on the plate (Fig. 4), in parasymphysial and more lateral positions, as in *Callorhinchus*. In later stages, the rods become more dominant, for example, in *Chimaera*, they are short (shallow, within the body

of the plate; Fig. 7D, F), particularly in the upper anterior dental plate, while in the posterior dental plate they comprise groups of ~~anterior~~ labial and ~~posterior~~ lingual units (Fig. 7D, E). In the posterior and lower dental plates of both taxa, rods are present along with the patch of irregular mineralization (Figs. 5B, C, F, H, J, 6D, F, K, O, S, 7D, H, J, O, R, ptch). The rods persist and develop in various locations, linked to different morphologies. For example, new rods can be added parasymphysially (in the anterior upper plates, Figs. 6D, F, 7K, R, T, white arrowheads) and to the lateral margin of the plate (e.g., Fig. 7R). As well, ~~dentine~~ whitlockin can be added to existing rods, such as on the posterior upper dental plate of *Chimaera*, where new ~~dentine~~ tissue ~~is being added to~~has formed at the medial margin of the parasymphyseal rod (Fig. 7J, L, arrowheads).

From this point, the rods have two developmental fates, depending on whether they are ~~more medial~~lingual or ~~more lateral~~labial in position. More ~~laterally~~labially, the morphology of rods is changed ~~replaced~~ at later growth stages into serial ovoid stacks ~~(preformed in the trabecular dentine)~~, with intermediate stages where ~~with intermediate stages~~~~seemingly where the~~ ovoids are not clearly separate entities (Figs. 5B, F, J, 7R, T). The rods are preformed in the trabecular dentine (Figs. 2D, 4C), as are the ovoids (Smith et al., 2019); the intermediate ovoid morphologies suggest a transformation of the trabecular dentine from rod to preformed ovoid shapes. ~~Medially~~Lingually, by comparison, the change involves regenerative growth rather than overall replacement, indicated by ~~the additional dentine~~ whitlockin being added to the rods, hence changing the morphology of the visceral rod surface. This visceral surface is crossed by distinct grooves (e.g., Fig. 6Q), representing the course of the associated vasculature, while Figure 7T shows an irregular medial rod in *Chimaera*, including curved margins and small circular openings. These are interpreted as dentine growing around blood vessels, as described above for *Callorhinchus*.

Thus, it appears that although the morphology of the adult holocephalan dental plates differs in the Callorhinchidae and Chimaeridae, these distinct morphologies derive in early development from simple rod-like structures. Only limited growth stages of the Rhinochimaeridae (e.g., *Harriotta*) were available (Smith et al., 2019), but from what was ~~seen~~observed, it appears that that ovoids and tritors in this group share a similar development. The elongate rods are first deposited within the elevated folds that cross the oral surface of the dental plate. The dentine rods occur in all dental plates, and eventually

are replaced by the ovoids, or grow to develop into the tritoral pads. An important feature in the continually growing dental plate is that medial (or parasymphysial) serial folds remain, but are restricted to this location as the only region where growth can be initiated ~~(Smith et al., 2020)~~in contact with oral epithelium (Smith et al., 2020: fig. 7).

As noted, whitlockin is deposited into morphological spaces that form within the ~~dentine framework~~growing scaffold of the trabecular dentine of the ~~dental~~ plates (Smith et al., 2019). This suggests that the transition between these rod-like and ovoid and tritor morphologies results from a change in the vascular, capsular spaces within the trabecular dentine. These changes appear to be gradual, with rods with irregular ~~dentine~~ whitlockin margins (Fig. 5F, G) ultimately being replaced by more regular, discrete and rounded ovoids. With respect to the tritoral pad, the first changes occur on the visceral surface (Fig. 6Q), including grooves for the blood vessels in the whitlockin (Fig. 7T) that subsequently develop completely around vascular canals to form the characteristic tritoral pad morphology. Following observations in *Harriotta*, we predict these changes in whitlockin morphology are preceded by changes in the framework dentine (Smith et al., 2019: fig. 2D, E).

While the rod grows and persists in the Chimaeridae before transforming into the tritoral pad, this appears to occur more quickly in the Callorhinchidae (Fig. 2K, L). In both families, the dentine of the rod tissue developing within the folds at the oral surface expands to surround the vascular canal space, although in the Chimaeridae there is a stage where the canals more clearly form as grooves on the dentine rod (e.g., Fig. 6Q). In later growth stages, the dental plates in the Callorhinchidae comprise only the tritoral pads; rods do not persist, and ovoid series do not form. Evidence from the fossil record shows that stem-group holocephalan dental plates are characterized by tritoral pads and ovoids (Johanson et al., 2020), suggesting retention of this morphology in the families Chimaeridae and Rhinochimaeridae (*Harriotta*, Smith et al., 2019) and loss in the Callorhinchidae.

*Histology of replacement growth of whitlockin*

The histology of sections through the developing dental plates of 75mm embryos of *Callorhinchus milii* (Kemp, 1984; Smith et al., 2020: fig. 7e) shows that the

hypermineralized dentine formed beneath the embryonic folds of the outer layer of dentine (Schaunisland, 1903, pl. 21; fig. 156), as described above. This tissue was called pleromin (Kemp, 1984), following the concept of an infilling tissue type, with specialised cells (pleromoblasts) forming this in embryonic stages, within spaces in normal dentine, i.e., as a functional term, from studies in ptyctodontids (placoderms) and chimaeroids (chondrichthyans; Ørvig, 1980, 1985). Recently, however, the same tissue was instead named whitlockin in extant chimaeroids, in reference to its composition, reflecting the unique form of mineral with high amounts of magnesium, as well as very different microstructural details of formation during mineralization (Smith et al. 2019, figs. 3, 5, cbs), with enlarged cell spaces aligned in a row at the formative surface (Fig. 9E; Smith et al., 2019: figs. 4, 6, 15). This composition ~~was~~ is unlike the pleromic tissues forming collagen-based, hydroxyapatite-containing hypermineralized dentine. Nevertheless, the cells forming whitlockin (Fig. 9E) are ~~described~~ proposed as ~~originating from~~ the odontoblast cell type, ~~as seen by differences~~but with clear differences between the whitlockin and the trabecular dentine (Smith et al., 2019, figs. 4F, 6D-F). At the embryonic stages of plate development ~~(Kemp 1984)~~ both cell types are presumed to be ~~illustrated~~present (e.g., mineralizing rods, Figs. 2, 4; Kemp, 1984), and in adult tissue, whitloblast cell body spaces form a layer at the surface, connected with the massive number of ramifying tubules within the forming whitlockin, as illustrated in Figure 9E, this arrangement is coincident with those in histological sections through embryonic plates (Didier et al., 1994: fig. 12). In high magnification histology, odontoblasts have fewer tubules, arranged very irregularly ~~(Smith e al., 2019, figure 4)~~, these contrast readily with the extremely large spaces for whitloblasts on the surface of ovoid and tritoral tissue along with the extensive, very numerous tubules (Smith et al., 2019: figs. 4E, F, td versus ov, tu).

The arrangement of the whitlockin in relation to our observations of the changing morphologies of tritoral dentine from embryo to adult and between species is interpreted in a model (Fig. 9F) showing detailed cellular control of this specialized dentine production in a tritor, ~~The arrow in Figure 9D shows a~~through two adjacent vascular tubes, in a block section (~~two~~identical tubes ~~shown~~ , white arrow, ~~diagramatically in~~ Fig. ~~9F~~9D), ~~These are~~ normal to the oral surface. Schematically, ~~diagram (Fig. 9F)~~ whitloblasts are the larger cells in the layer lining the forming whitlockin, whereas odontoblasts are represented by the

graded, reduced size cell layer forming the peritubate dentine. ~~Within the trabecular framework of normal dentine, these specialized odontoblasts, or whitloblasts, deposit the high-density mineralized whitlockin.~~ These cells are joined together to form an active membrane on the surfaces as they generate enormous numbers of tubules within the forming and completed whitlockin tissue (Fig. 9E, F; Smith et al., 2019: figs. 4F, 6E, F). In the tritoral pads (Fig. 9A–C), whitloblasts reduce in height, become odontoblasts, then form less mineralized peritubate dentine to enclose the blood vessels ~~in a regular arrangement, resulting~~ in a regular arrangement, resulting in the punctate surfaces (Fig. 9F, orange tissue, smaller odontoblasts). Changes from juvenile to adult in the extent of this punctate surface are observed in the whole lower dental plate of a younger individual (Fig. 9A), along with an adult tritoral pad that has been worn anteriorly and exposed at the oral surface (Fig. 9B, black arrowhead). In virtual, horizontal sections through this same region, new, less mineralized dentine has formed ~~is deposited~~ around the vascular tubes in the still-developing, unexposed part of the tritoral pad (Fig. 9C, small white arrows, darker region).

Cells surrounding each vascular canal are proposed to control the physiology of ion transport, in and out of the cellular membrane responsible for all dentine formation (pink cells, Fig. 9F). In the intertubate dentine (ITD), a regular arrangement of vascular canals results in the punctate surface, each with a thin layer of the less mineralized tissue known as peritubate dentine (PTD; Fig. 9C, F). The vascular proximity within this arrangement ensures a regular massive supply of materials to the cells, in particular, the specialized whitloblasts as a continuous lining to the growth surface~~, shown here as a continuous layer~~. This layer forms a cellular membrane that controls influx and stability of Ca, P and Mg ions of the intertubate dentine (whitlockin). Processes outlined in this model can be related to tissue histology in the dental plates of both fossil (Fig. 9D), and extant forms (Fig. 9E; Smith et al., 2019: figs. 6D, E, F). ~~In the extant forms, high resolution micrographs of the formative, mineralizing surfaces between the vascular tubes (Fig. 9E) demonstrate cell spaces at the forming front leading to the massive numbers of tubulesalong with reduced cells lining this front that are forming the peritubate dentine.~~

We have proposed that this unusual hypermineralized dentine (whitlocki~~i~~n) with very high levels of Mg in the intertubate region (Ishyama, 1991; Smith et al., 2019: figs. 14, 15) must have cellular control in the form of this tightly bound membrane, with the processes

of the cells continuing into the peritubate dentine, less mineralized and with less Mg (Fig. 9F). We suggest two possible ~~theories~~ hypotheses for this control, to allow for change in the mineral content, and as a consequence, the change in morphology due to the differential hardness within dentine plates. First, either the same cells change their activity, i.e., odontoblasts first change to whitloblast activity, then revert to odontoblast-type activity (Fig. 9F) when lining the vascular tubes; or, second, a subset of cells from the embryonic ectomesenchyme ~~stays~~ remain in the pulp and differentiate to make the new type dentine, whitlockin, onto the trabecular dentine frame. To test ~~these two~~the second hypotheses~~his proposal~~ would ~~need~~require future experimental investigations (with vital cell labelling) on ~~impossibly rare~~ embryos of extant forms, ~~but would be reasonable on~~for example *Callorhincus milii* where embryos have been obtained previously (Johanson et al. 2015). That is, ~~it requires~~ lineage tracing is required from early to late development to show that precursor ~~cells~~ whitloblasts have migrated onto the dentine surface and are then replaced by uncommitted stem-odontoblasts to make the peritubate dentine, linked by new cell processes into the surface of the whitlockin. But, because we observed the many, and thus ~~continuing~~ continuous, tubules that must stay connected to the ~~cells~~ cell processes making the tissues, we suggest this demonstrates the temporal continuity of the cells in the layer, ~~altering~~ alternating activity between ~~osteoblasts~~ odontoblasts and whitloblasts, changing back to ~~osteoblasts~~ odontoblasts to secrete the less mineralized ~~dentine~~ dentine, with fewer tubules, located around the vascular tubes (Fig. 9F); these observations favour the first hypothesis. This is a physiological interpretation from cell type spaces and quantitative mineralogy that shows differences between the species so far investigated in our published studies.

## Conclusions

The distribution of the extra hard dentine as whitlockin

## ~~Conclusions~~

~~The distribution of the extra hard dentine as whitlockin~~ within the trabecular dentine of the dental plate compensates for the evolutionary loss of separate teeth on the jaws of extant holocephalans. The different hardness of these tissues, dependent on the secretion of whitlockin by specialist odontoblastic cells, results in differential wear at the oral surface.

where different morphologies are found between young and adult individuals. This wear is compensated by new formation of dentine aborally where cells from the visceral pulpal tissues differentiate and contribute to continuous renewal of the surrounding trabecular dentine and whitlockin, ~~all formed~~still in specific patterns that we have demonstrated ~~in this paper,~~ change through ontogeny to the adult pattern.

We have observed that the dental plate is supplied with a rich vasculature, the visceral plate margin is open for a vascularised pulp tissue and at early ontogenetic stages large pores open into the dental plate to facilitate this. This suggests that in the pulpal tissue the pre-odontoblast cells differentiate from neural crest-derived ectomesenchyme (as all vertebrate teeth have been shown to derive from neural crest, including fish; Kundrát et al., 2008), first into odontoblasts then whitloblasts. Cells making the dentine of mammalian dentine have demonstrated the link between neural crest, odontoblasts, and vascular tissue. However, odontogenic cells must be continuously renewed in the pulp chamber, from stem cells, nerves, and vascular tissue at the visceral surfaces (Smith et al., 2020a, b).

Within the Callorhinchidae and the Rhinochimeridae + Chimaeridae, the morphology of the dental plate is strikingly different and important taxonomically. Although similarities in early development include rods, other adult surface morphologies (ovoids, tritoral pads, patches) take different arrangements (Stahl, 1999), formed specifically within a trabecular dentine as different sites of whitlockin development, this includes differences between each of three plates on each ~~side~~ of the jaws (Smith et al., 2019: figs. 14, 15). Nevertheless, these taxa show similarities in early development, with the first ~~hypermineralized dentine~~whitlockin deposited within folds at the medial, aboral~~oral~~ surface; we suggest this folding is a mechanism related to dentine deposition within the outer dentine layer of the holocephalan dental plate, ~~being maintained medially and~~ related to ongoing deposition of all dentine types aborally (Smith et al., 2020b, fig. 7).

Especially, we conclude that the novel dentine whitlockin, responsible for the morphologies described in this paper, is only present in holocephalans and evolved in the absence of teeth through a new activity of the odontoblast cells, functioning as whitloblasts, transformed from those making the trabecular dentine that surrounds the whitlockin. The layer of the whitloblast cells lining the tubate dentine, once reduced in size, transform into odontoblasts to form the peritubate, ordinary dentine. Here they continue to monitor the

lower levels of minerals at a slower rate of growth and lower levels of Mg. As noted, it is axiomatic that the cells making the dentine of all vertebrate teeth are derived from neural-crest (ectomesenchyme; Kundrát et al., 2008). The ability of these cells to ~~these have persisted in the absence of teeth and form this specialized~~ make trabecular dentine~~; the ability o f the odontoblasts to~~ and transform into whitloblasts, then reverse the process, reflects the pluripotency of the ubiquitous neural crest.

**Acknowledgements**

We would like to thank Marine Scotland, the crew of the MRV Scotia and Francis Neat and Finlay Burns who provided us with many of the specimens used here, whilst Clive Trueman and Chris Bird (University of Southampton) both helped obtain specimens and helped with general discussions of chimaeroid biology.

**Author Contributions**

ZJ, MMS and CU conceived the project, EM reconstructed CT-data during a 3-month research visit to the NHM, BC and VF CT-scanned specimens. All authors discussed the results and all contributed to the manuscript.

**Conflicts of Interests**

None.

**Data Availability Statement**

Rotatable 3D mesh model .stl files are available at the NHM Data Portal: data.nhm.ac.uk/dataset/ontogenetic-development-of-the-holocephalan-dentition.

**References**

Bory de Saint-Vincent, J.B.G.M. (1823). *Dictionnaire Classique d'Histoire Naturelle, Paris*, **3**, 61–62, 1.

Capello F. B. 1868. Catalogo dos peixes de Portugal que existem no Museu de Lisboa. *Jornal de Sciencias Mathematicas, Physicas e Naturaes* **2**, 51 – 63.

651 Dean, B. (1906). Chimaeroid fishes and their development. *Carnegie Institute of*
652 *Washington*, 32, 1-194.
653 Dean, B. (1909). Studies on fossil fishes (sharks, chimaeroids and arthrodires). *Memoirs of*
654 *the American Museum of Natural History* 9, 211–287.
655 Didier, D.A. (1995). Phylogenetic systematics of extant chimaeroid fishes (Holocephali,
656 Chimaeroidei). *American Museum Novitates* 3119, 1–86.
657 Didier, D.A. (2004). Phylogeny and classification of extant Holocephali. In: J.C. Carrier,
658 J.C., Musick, J.A. and Heithanus, M.R. (Eds.) *Biology of Sharks and their Relatives*.
659 London, UK: CRC Press, pp. 115–135.
660 Didier, D.A., Stahl, B.J. and Zangerl, R. (1994). Development and growth of compound
661 tooth plates in *Callorhinchus milii* (Chondrichthyes, Holocephali). *Journal of*
662 *Morphology* 222, 73–89.
663 Duffin, C.J. and Delsate, D. (1995). New record of the Early Jurassic myriacanthid
664 holocephalan *Myriacanthus paradoxus* AGASSIZ, 1836 from Belgium. *Belgian*
665 *Geological Society Professional Paper* 278, 1–9.
666 Garman, S. (1904). The chimaeroids (Chismopnea Raf., 1815; Holocephala Müll., 1834),
667 especially *Rhinochimaera* and its allies. *Bulletin of the Museum of Comparative*
668 *Zoology* 41, 245–272.
669 Hardy, G.S. and Stehmann, M.F.W. (1990). A new deep-water ghost shark, *Hydrolagus*
670 *pallidus* n. sp. (Holocephali, Chimaeridae), from the eastern North Atlantic, and
671 redescription of *Hydrolagus affinis* (de Brito Capello, 1867). *Archiv für*
672 *Fischereiwissenschaft* 40, 229-248.
673 Iijima, M. and Ishiyama, M. (2020). A unique mineralization mode of hypermineralized
674 pleromin in the tooth plate of *Chimaera phantasma* contributes to its
675 microhardness. *Scientific Reports* 10**,** 18591. https://doi.org/10.1038/s41598-020-
676 75545-0
677 Ishyama, M. and Sasagawa, A.J. (1984). The inorganic content of pleromin in tooth plates
678 of the living Holocephalan, *Chimaera phantasma*, consists of a crystalline calcium
679 phosphate known as ß-$Ca_3(PO4)_2$ (whitlockite). *Archives of Histology and Cytology*
680 47, 89–94.

Ishiyama, M., Yoshie, S., Teraki, Y. and Cooper, E.W.T. (1991). Ultrastructure of pleromin, a highly mineralized tissue comprizing crystalline calcium phosphate known as Whitlockite, in Holocephalian tooth plates. In: Suga, S. and Nakahara, H. (Eds). *Mechanisms and Phylogeny of Mineralization in Biological Systems*. Tokyo: Springer-Verlag. pp. 453–457.

Johanson, Z., Boisvert, C., Maksimenko, A., Currie, P. and Trinajstic, K (2015). Development of the synarcual in the Elephant Sharks (Holocephali; Chondrichthyes): Implications for vertebral formation and fusion. *PLoS ONE* 10(9), e0135138. https://doi.org/10.1371/journal.pone.0135138

Johanson, Z., Manzanares, E., Underwood, C.J., Healy, C., Clark, B. and Smith, M.M. (2020). Evolution of the dentition in holocephalans (Chondrichthyes) through tissue disparity. *Integrative and Comparative Biology* icaa093, https://doi.org/10.1093/icb/icaa093

Johanson, Z., Manzanares, E., Underwood, C.J., Clark, B, Fernandez, V. and Smith, M.M. (2020). Ontogenetic development of the holocephalan dentition: Morphological transitions of dentine in the absence of teeth. Data set including .stl files. *NHM Data Portal: data.nhm.ac.uk/dataset/ontogenetic-development-of-the-holocephalan-dentition*.

Kemp, A. (1984). A comparison of the developing dentition of *Neoceratodus forsteri* and *Callorhynchus milii*. *Proceedings of the Linnean Society of New South Wales* 107, 245–262.

Kundrát, M., Joss, J.M.P. and Smith, M.M. (2008). Fate mapping in embryos of *Neoceratodus forsteri* reveals cranial neural crest participation in tooth development is conserved from lungfish to tetrapods. *Evolution and Development* 10, 531–536.

Linnaeus, C. (1785). *Systema naturae per regna tria naturae :secundum classes, ordines, genera, species, cum characteribus, differentiis, synonymis, locis* (in Latin) (10th ed.). Stockholm: Laurentius Salvius.

Lund, R. (1977). New information on evolution of the bradyodont Chondrichthyes. *Fieldiana Geology* 33, 521–539.

Lund, R. (1986). The diversity and relationships of the Holocephali. In: Uyeno, T., Arai. R., Taniuchi, T. and Matsuura, K. (Eds.) *Proceedings of the Second International Conference on Indo-Pacific Fishes, Tokyo*. Tokyo: lchthyological Society of Japan, pp. 97–106.

Lund, R. (1988). Holocephali. In: Russell, D.E., Santoro, J.P. and Sigogneau-Russell. D. (Eds). *Teeth Revisited. Proceedings of the VII International Symposium on Dental Morphology, Paris*. Memoirs of the Museum National d'Histoire Naturelle Paris 53C, 195–205.

Lund, R. and Grogan, E. (1997). Relationships of the Chimaeriformes and the basal radiation of the Chondrichthyes. *Reviews in Fish Biology and Fisheries* 7, 65–123.

Miletich, I. and Sharpe, P.T. (2004). Neural crest contribution to mammalian tooth formation. *Birth Defects Research C Embryo Today: Reviews* 72, 200–212.

Ørvig, T. (1967). Phylogeny of tooth tissues: evolution of some calcified tissues in early vertebrates. In: Miles, A.E.W. (Ed.) *Structural and Chemical Organization of Teeth*. New York, NY: New York Academic Press. pp. 45–110.

Ørvig, T. (1985). Histologic studies of ostracoderms, placoderms and fossil elasmobranchs. 5. Ptyctodontid tooth plates and their bearing on holocephalan ancestry: the condition of chimaerids. *Zoologica Scripta* 14, 55–79.

Patterson, C. (1965). The phylogeny of the chimaeroids. *Philosophical Transactions of the Royal Society B* 249, 101–219.

Patterson, C. (1992). Interpretation of the toothplates of chimaeroid fishes. *Zoological Journal of the Linnean Society* 106, 33–61.

Popov, E.V. (2003). A new genus of Elephant fishes (Holocephali: Callorhinchidae) from the Upper Callovian of the Volga Region near Saratov, Russia. *Paleontological Journal* 37, 59–66.

Schauinsland, H. (1903.) Beitrage zur Entwicklungsgeschichte und Anatomie der Wirbeltiere. I. *Sphenodon*, *Callorhynchus*, *Chamaleo*. Zoologica 16, 1–98.

Stahl, B.J. (1999). *Handbook of Paleoichthyology. Volume 4. Chondrichthyes III. Holocephali*. München: Verlag Dr Friedrich Pfeil.

Smith, M.M., Underwood, C., Goral, T., Healy, C. and Johanson, Z. (2019). Growth and mineralogy in dental plates of the holocephalan *Harriotta raleighana*

(Chondrichthyes): novel dentine and conserved patterning combine to create a unique chondrichthyan dentition. *Zoology Letters* 5, 11.

Smith, M.M., Manzanares, E., Underwood, C.J., Healy, C., Clark, B. and Johanson, Z. (2020). Holocephalan (Chondrichthyes) dental plates with hypermineralized dentine as a substitute for missing teeth through developmental plasticity. *Journal of Fish Biology* 97, 16-27.

Zangerl, R. (1981). Handbook of Paleoichthyology. Volume 3A: Chondrichthyes I. München: Verlag Dr Friedrich Pfeil. 113 pp.

Zangerl, R., Winter, H.F. and Hansen, M.C. (1993). Comparative microscopic dental anatomy in the Petalodontida (Chondrichthyes, Elasmobranchii). *Fieldiana Geology* 26, 1-42.

**Figure Captions**

**Figure 1** Phylogenetic relationships of the Chondrichthyes, and the sister-group relationship between Elasmobranchii (sharks, rays) and the Holocephali.

**Figure 2 Family Callorhinchidae, *Callorhinchus milii.*** (A–G), embryonic or neonate specimen, Western Port bay, Victoria, Australia. (A–D), upper dentition, anterior and posterior upper dental plates in (A) oral view, with folds crossing the posterior dental plate; (B) labial view, black arrowheads mark the position of openings along the labial margin of the posterior dental plate; (C) visceral view, white arrow and black arrowheads mark distinct lamina forming on the anterior, and posterior, dorsal plates, respectively; (D) virtual section through the posterior dental plate and folds shown in (A), white arrow indicates section through the fold and dentine being deposited within; (E–G), lower dentition, (E) lower dental plate in oral view, folds cross the plate surface as in the upper posterior plate; developing dentine is visible where the folds are open posteriorly (white arrowheads); (F) virtual section through lower dental plate and folds shown in (E), white arrows indicate section through the folds and dentine being deposited within; (G) visceral view, distinct lamina absent (black asterisk indicates smooth face of the plate that is visible. (H–L), early growth stage, Western Port bay, Victoria, Australia. (H) labial view of upper

773 and lower dental plates; (I) upper dental plates in oral view, black arrowheads indicate
774 position of folds on the posterior dental plate, curved folds on anterior dental plate as well
775 (compare to Fig. 1A); (J) upper dental plates in oral view, black arrowheads show
776 developing lamina on the posterior dental plate, white arrowheads show developing lamina
777 on anterior plates; (K) lower dental plate in oral view, black arrowheads indicate position of
778 folds (compare to Fig. 1E), false color red indicates more highly mineralized dentine,
779 absent in Fig. 1A–E; (L) more highly mineralized dentine separated virtually from the rest
780 of the dental plate. White arrows show position of dentine developing around vascular
781 canal spaces. (M–O), dentition of an adult, uncatalogued NHM Palaeo specimen (Patterson,
782 1965), posterior upper dental plate in (M) oral, (N) visceral views. In (N), white arrowheads
783 mark well developed lamina, compare to Fig. 1C, J; (O) virtual section through dental plate
784 showing more highly mineralized dentine (white) surrounding vascular canals, along with
785 the oral and aboral territories, related to the lamina (Didier et al., 1995). Abbreviations: a,
786 anterior; ADP, anterior dental plate; fo, fold crossing plate surface; LDP, lower dental
787 plate; PDP, posterior dental plate; trab, trabecular dentine; tri, tritoral pad, vasc, vascular
788 canals. Scale bar H–K= 2 mm; N, O = 1 cm.
789
790 **Figure 3 Family Callorhinchidae, *Callorhinchus callorhinchus*.** (A–G), skull of smaller
791 adult, commercial supplier, Uruguay. (A–C)**,** upper dental plates in (A) oral view; (B) with
792 hypermineralized dentine virtually separated from the surrounding dental plate, tritors well-
793 developed in anterior and posterior plates; (C) anteroposterior virtual section through dental
794 plates showing more highly mineralized dentine (white) surrounding vascular canals, along
795 with the oral and aboral territories. (D–F), lower dental plate in (D) oral view; (E) with
796 hypermineralized dentine virtually separated from the surrounding dental plate, tritors well-
797 developed and mineralization occurring at the anterior margin; (F) transverse section
798 through the lower dental plate; (G) anteroposterior virtual section through dental plates
799 showing more highly mineralized dentine (white) surrounding vascular canals, along with
800 the oral and aboral territories. (H–M), **s**kull of larger adult, commercial supplier, Uruguay.
801 (H–J), upper dental plates in (H) oral view; (I) with hypermineralized dentine virtually
802 separated from the surrounding dental plate, tritors well-developed in anterior and posterior
803 plates; (J) anteroposterior virtual section through dental plates showing more highly

804 mineralized dentine (white) surrounding vascular canals, along with the oral and aboral
805 territories. (K–M), lower dental plate in (K) oral view; (L) with hypermineralized dentine
806 virtually separated from the surrounding dental plate, tritors well-developed and
807 mineralization occurring at the anterior margin; (M) anteroposterior virtual section through
808 dental plates showing more highly mineralized dentine (white) surrounding vascular canals,
809 along with the oral and aboral territories. Abbreviations: As in Figure 2, also, abor, aboral
810 region of dental plate; l.jaw.cart, lower jaw cartilage; oral, oral region of dental plate. Scale
811 bar= 1 cm.
812
813 **Figure 4 Family Chimaeridae, *Hydrolagus affinis*.** (A–I), BMNH2003.11.16, small
814 juvenile, UK. (A) lateral view of head; (B) labial view of upper and lower dental plates in
815 association (softer tissues including jaw cartilage removed virtually); (C) dorsal (visceral)
816 view of upper and lower dental plates, in association with, and overlying, the lower dental
817 plates. On left side of the image, false colour red indicates the anterior upper dental plate
818 and blue the posterior upper dental plate. Green represents the lower dental plate. On the
819 right side of the image, openings (pores) are visible on the margins of the upper dental
820 plates, and folds on the lower plate (compare to Fig. 2); (D) dental plates in occlusion,
821 upper plates in visceral view, oral margin of lower dental plates visible, with different
822 segmentation parameters compared to (C). Open margins visible on the anterior and
823 posterior dental plates. (E) upper dental plates in oral view, showing parasymphysial folds
824 and more posterior pores; (F) modified segmentation settings showing outer dentine layer
825 (dark grey) and inner cavity (light) grey; G) lower dental plates in oral view; (H) virtual
826 transverse section through lower plates, showing openings in folds on the oral surface; I)
827 virtual section through fold, showing dentine rod within. Abbreviations as in previous
828 plates, also: fo.op, opening in dental plate fold; idl, inner dentine layer; odl, outer dentine
829 layer; op, open margin of dental plate; p.fo.op, opening in parasymphysial dental plate fold.
830 Scale bar A–C= 1 cm; D=5mm; E= 3mm; F–I= 2.5mm.
831
832 **Figure 5 Family Chimaeridae, *Hydrolagus affinis*.** (A–C), small juvenile, Scotland. (A,
833 B) upper and lower dental plates in association, lateral view, (B) with surrounding tissues
834 removed virtually to show mineralized rods, ovoids and patches; (C) upper and lower

dental plates in association, anterior view, false coloured to show mineralized elements (red) and surrounding dentine (green). (D–J)**,** larger juvenile, Scotland. (D), skull and lower jaw, lower jaw and upper and lower dental plates in lateral view; (E–H) upper dental plates in oral view, (F–H) plates virtually dissected to show mineralized rods, ovoids and patches; (I, J) lower dental plate, oral view; (J) surrounding dentine removed virtually to show mineralized dentine forming rods and patches, asterisks indicate position of elongate rods associated with folds on the dental plate surface. Abbreviations as in previous plates, also ptch, patch of irregular mineralization; rd/tri, rod that will develop into tritor in later growth stages. Scale bar= 0.5 cm.

**Figure 6 Family Chimaeridae** (A–K) *Hydrolagus pallidus*, large adult, Scotland. (A, B) jaws and dental plates in (A) anterior; (B) lateral views. (C–I) upper anterior and posterior dental plates, in oral view; (D–F) surrounding tissue virtually removed to show rods, ovoids, patches for (E) anterior, (F) posterior plates, arrows and arrowheads indicate newly developing rods. (G–I) virtual sections through upper dental plates to show developing ovoids (G, H, transverse section; I, longitudinal section), white arrows indicate aboral territory (compare to Fig. 1). (J, K) lower dental plate in (J) oral view; (K) surrounding tissue virtually removed to show rods, ovoids and patches. (L–S) Chimaeridae indet, skull of probable adult, commercial supplier, probably Philippines. Skull, jaws and dental plates in (L) anterior; (M) lateral views; (N–Q) upper anterior and posterior dental plates in oral view; (O–Q) surrounding tissue virtually removed for anterior and posterior plates, arrows indicate new parasymphysial element added, arrowheads showing position of developing tritor in the posterior dental plate; (P, Q) hypermineralized tissue in (P) oral and Q) visceral views, arrowheads show position of developing tritor including grooves marking the visceral surface. (R, S) lower dental plate in (R) oral view; (S) with surrounding tissue virtually removed. Abbreviations as in previous Figures. Scale bar=1.5cm

**Figure 7 *Chimaera monstrosa*** (A–H) *Chimaera monstrosa* juvenile, Scotland. Skull, jaws and dental plates in (A) anterior; (B) lateral views (anterior to left). (C–F) upper anterior and posterior dental plates in oral view; (D–F) surrounding tissue virtually removed for anterior and posterior plates to expose rods and patches, including in the (E) posterior and

(F) anterior dental plates. G, H) lower dental plate in G) oral view; H) surrounding tissue virtually removed. (I–O) *Chimaera monstrosa* juvenile, Scotland, upper and lower dental plates; (I–M) upper plates in oral view; (J–M) surrounding tissue virtually removed for anterior and posterior plates; (L, M) hypermineralized dentine in the posterior dental plate shown in (L) oral and (M) visceral views. Arrowheads indicate new dentine being added to the parasymphysial rod (J, M), new parasymphysial rod forming (K); arrows indicate grooves and circular openings developing on the surface of the rod (L); asterisks indicate second smaller, more anterior rod forming (L, M); (N, O) lower dental plate in (N) oral view; (O) surrounding tissue virtually removed. (P–T) *Chimaera monstrosa*, immature male (very small claspers), Scotland. Skull and upper dental plates in (P) lateral view (anterior to left). (Q–T) upper anterior and posterior dental plates in (Q) oral view; (R) surrounding tissue virtually removed for anterior and posterior plates and for (S) anterior and (T) posterior plates. Arrowheads indicate new dentine being added to the parasymphysial rod (R), paired arrows mark new parasymphysial rod forming (R, S); single arrows indicate grooves and circular openings developing on the surface of the rod (T). Abbreviations as in other Figures. Scale bar = 5 mm.

**Figure 8 *Chimaera* sp.** (A–G) *Chimaera* sp. indet., juvenile, commercial supplier, Taiwan. (A) skull, jaws, dental plates, part of the body including dorsal fin and spine in lateral view; (B, C) associated dental plates in (B) lateral and (C) anterior views. (D, F), upper anterior and posterior dental plates in oral view; (F) surrounding tissue virtually removed from both plates; (E, G) lower dental plate, (G) surrounding tissue virtually removed. Arrows (F) indicate anterior part of tritoral pad lacking opening for vascular canals. Scale bars= 4mm (D, F); 3mm (E).

**Figure 9** (A-C), *Harriotta raleighana*; tritoral hypermineralized dentine formation, to illuminate tissue structure of the plate morphology, in (A) lower jaw of a younger individual, CT-scan 3D rendered of tritoral tubate dentine surface (arrow; from Smith et al. 2019: fig. 16B). (B, C) adult upper jaw tritoral pad, (B) CT-scans 3D density rendered, from mature whitlockin at the oral, exposed surface, to forming whitlockin more basally (arrow); (C) a horizontal virtual section of the same region with many regular vascular

tubes on the exposed surface, in the forming tissue these have rings of less dense peritubate dentine (white arrows; Smith et al., 2019: fig. 17). (D) *Strebelodus oblongus* (NHMUK PV P75426), sectioned dental plate shows fossil histology vertical to the punctate surface from oral to visceral, of tubate dentine in a tritor (arrow indicating two tubes), showings three zones of development of continuous mineralization, with parallel vascular tubes, normal to the oral surface, emanating from the larger vascular spaces in the trabecular dentine. (E) *Harriotta raleighana* (from Smith et al., 2019: fig. 6E), section of mineralized tissue of a tritoral pad, same plane as in (D) at high resolution, of cell spaces at the forming front, linked with a complex mass of increasingly fine diameter tubules emanating from the cell spaces in the first formed whitlockin, nearby many vascular capillaries (not shown but are represented in (F). (F) schematic, interpretive diagram of living tissue with cells responsible for whitlockin formation of a tritor as in (E), around two of the vascular tubes (e.g., arrow in D), comparable to those that make up all of this tissue (see surface views A–C). ~~It is envisaged that in life the cells form a tight membrane that can control active influx of minerals to the rapidly mineralizing dentine as whitlockin, as can the layer of the reduced whitoblast cells at a lower rate; once transformed into odontoblasts they form the peritubate 'softer' dentine; these cells continue to monitor the lower levels of minerals at a slower rate of growth and lower levels of Mg (Smith et al. 2019), as a diagrammatic interpretation of cellular activity.~~ Images in Figure 9A, E reproduced under Creative Commons attribution license, BMC (Smith et al. 2019: https://doi.org/10.1186/s40851-019-0125-3)

**Supplementary Information Figure 1.** *Hydrolagus affinis*, PTA-stained specimen showing soft tissues surrounding upper dental plates. (A) oral view of upper dental plates. (B) longitudinal section through the plates, white arrows indicating soft tissue epithelium surrounding all plate margins, which would include the lingual margin as well (in association with lingual ridges on the anterior dental plate).

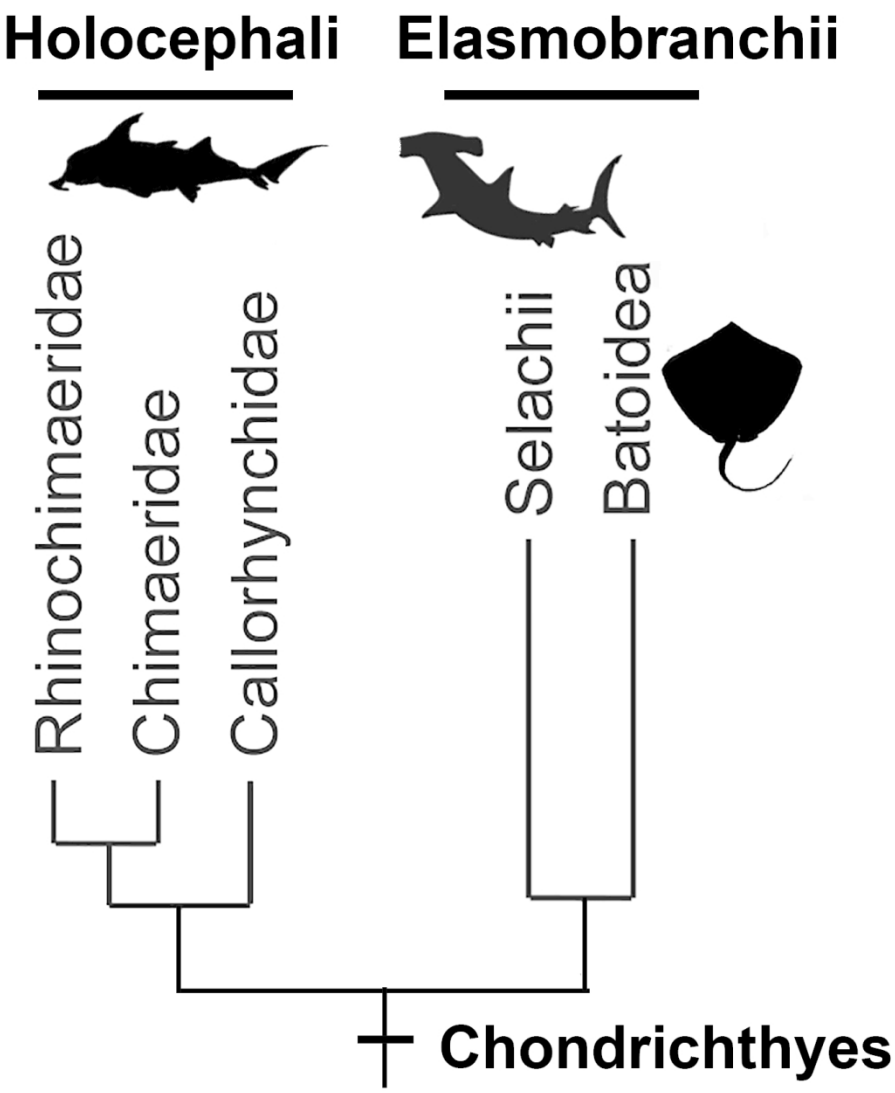


Figure 1 Phylogenetic relationships of the Chondrichthyes, and the sister-group relationship between Elasmobranchii (sharks, rays) and the Holocephali.

80x98mm (472 x 472 DPI)

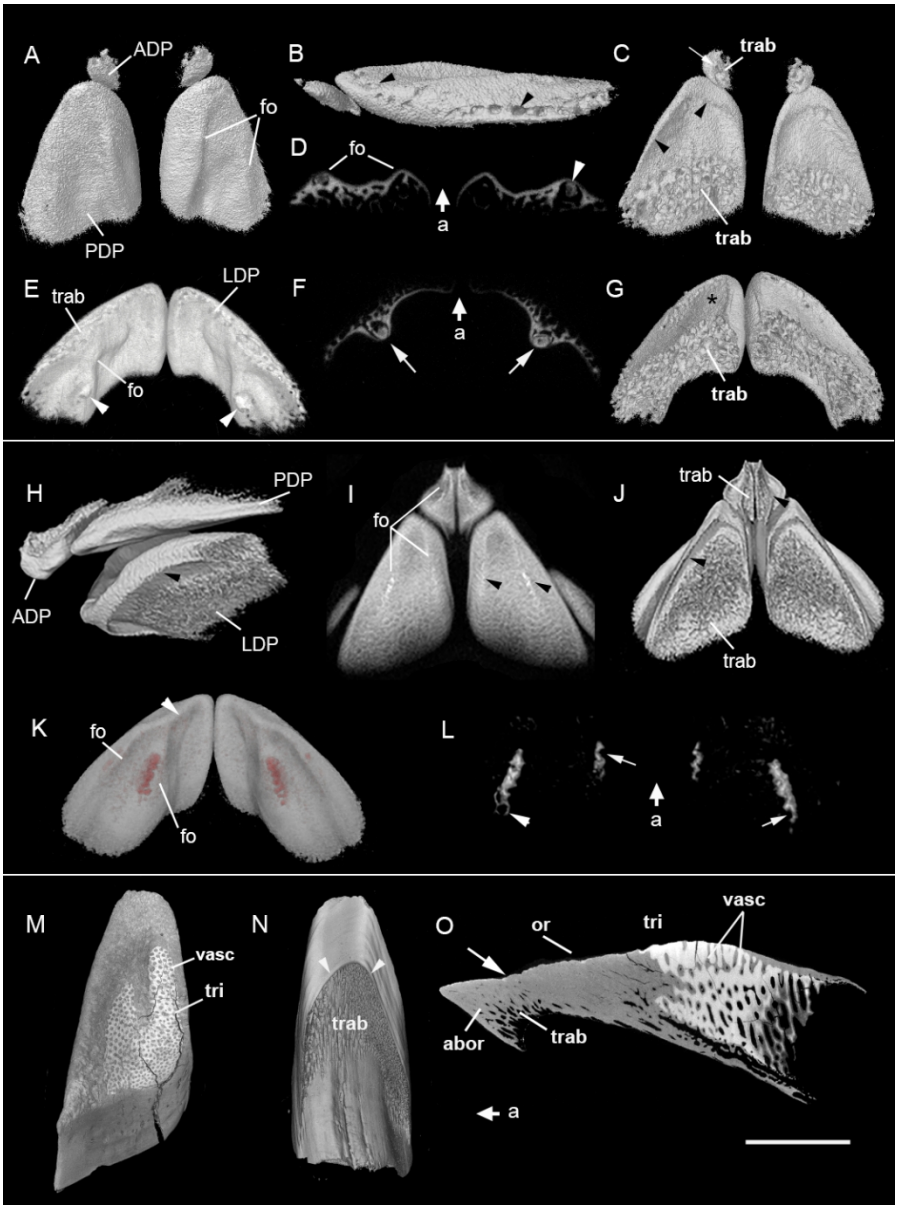


Figure 2 Family Callorhinchidae, Callorhinchus milii. (A–G), embryonic or neonate specimen, Western Port bay, Victoria, Australia. (A–D), upper dentition, anterior and posterior upper dental plates in (A) oral view, with folds crossing the posterior dental plate; (B) labial view, black arrowheads mark the position of openings along the labial margin of the posterior dental plate; (C) visceral view, white arrow and black arrowheads mark distinct lamina forming on the anterior, and posterior, dorsal plates, respectively; (D) virtual section through the posterior dental plate and folds shown in (A), white arrow indicates section through the fold and dentine being deposited within; (E–G), lower dentition, (E) lower dental plate in oral view, folds cross the plate surface as in the upper posterior plate; developing dentine is visible where the folds are open posteriorly (white arrowheads); (F) virtual section through lower dental plate and folds shown in (E), white arrows indicate section through the folds and dentine being deposited within; (G) visceral view, distinct lamina absent (black asterisk indicates smooth face of the plate that is visible. (H–L), early growth stage, Western Port bay, Victoria, Australia. (H) labial view of upper and lower dental plates; (I) upper dental plates in oral view, black arrowheads indicate position of folds on the posterior dental plate, curved folds on anterior dental plate as well (compare to Fig. 1A); (J) upper dental plates in oral view, black

arrowheads show developing lamina on the posterior dental plate, white arrowheads show developing lamina on anterior plates; (K) lower dental plate in oral view, black arrowheads indicate position of folds (compare to Fig. 1E), false color red indicates more highly mineralized dentine, absent in Fig. 1A–E; (L) more highly mineralized dentine separated virtually from the rest of the dental plate. White arrows show position of dentine developing around vascular canal spaces. (M–O), dentition of an adult, uncatalogued NHM Palaeo specimen (Patterson, 1965), posterior upper dental plate in (M) oral, (N) visceral views. In (N), white arrowheads mark well developed lamina, compare to Fig. 1C, J; (O) virtual section through dental plate showing more highly mineralized dentine (white) surrounding vascular canals, along with the oral and aboral territories, related to the lamina (Didier et al., 1995). Abbreviations: a, anterior; ADP, anterior dental plate; fo, fold crossing plate surface; LDP, lower dental plate; PDP, posterior dental plate; trab, trabecular dentine; tri, tritoral pad, vasc, vascular canals. Scale bar H–K= 2 mm; N, O = 1 cm.

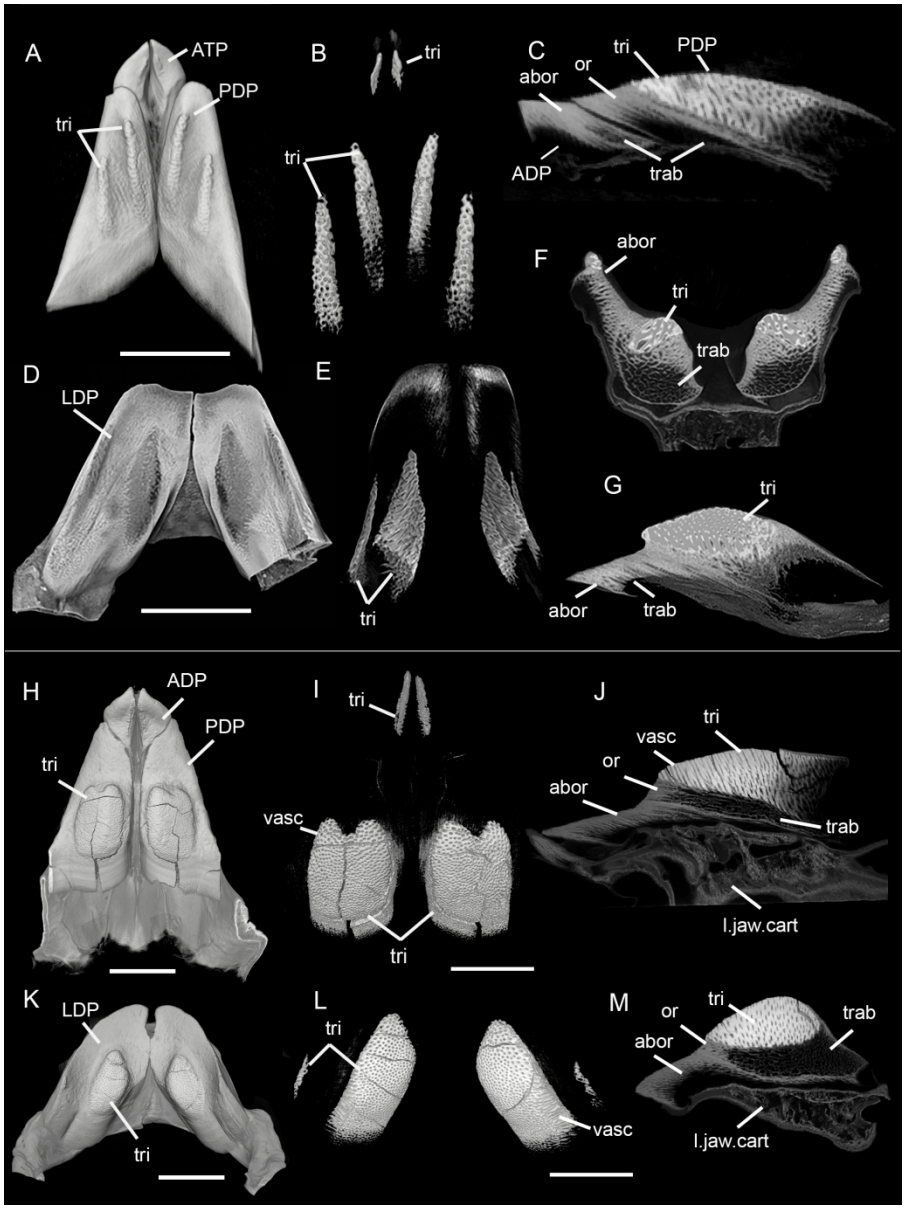


Figure 3 Family Callorhinchidae, Callorhinchus callorhinchus. (A–G), skull of smaller adult, commercial supplier, Uruguay. (A–C), upper dental plates in (A) oral view; (B) with hypermineralized dentine virtually separated from the surrounding dental plate, tritors well-developed in anterior and posterior plates; (C) anteroposterior virtual section through dental plates showing more highly mineralized dentine (white) surrounding vascular canals, along with the oral and aboral territories. (D–F), lower dental plate in (D) oral view; (E) with hypermineralized dentine virtually separated from the surrounding dental plate, tritors well-developed and mineralization occurring at the anterior margin; (F) transverse section through the lower dental plate; (G) anteroposterior virtual section through dental plates showing more highly mineralized dentine (white) surrounding vascular canals, along with the oral and aboral territories. (H–M), skull of larger adult, commercial supplier, Uruguay. (H–J), upper dental plates in (H) oral view; (I) with hypermineralized dentine virtually separated from the surrounding dental plate, tritors well-developed in anterior and posterior plates; (J) anteroposterior virtual section through dental plates showing more highly mineralized dentine (white) surrounding vascular canals, along with the oral and aboral territories. (K–M), lower dental plate in (K) oral view; (L) with hypermineralized dentine virtually separated from the surrounding dental

plate, tritors well-developed and mineralization occurring at the anterior margin; (M) anteroposterior virtual section through dental plates showing more highly mineralized dentine (white) surrounding vascular canals, along with the oral and aboral territories. Abbreviations: As in Figure 2, also, abor, aboral region of dental plate; l.jaw.cart, lower jaw cartilage; ¬oral, oral region of dental plate. Scale bar= 1 cm.

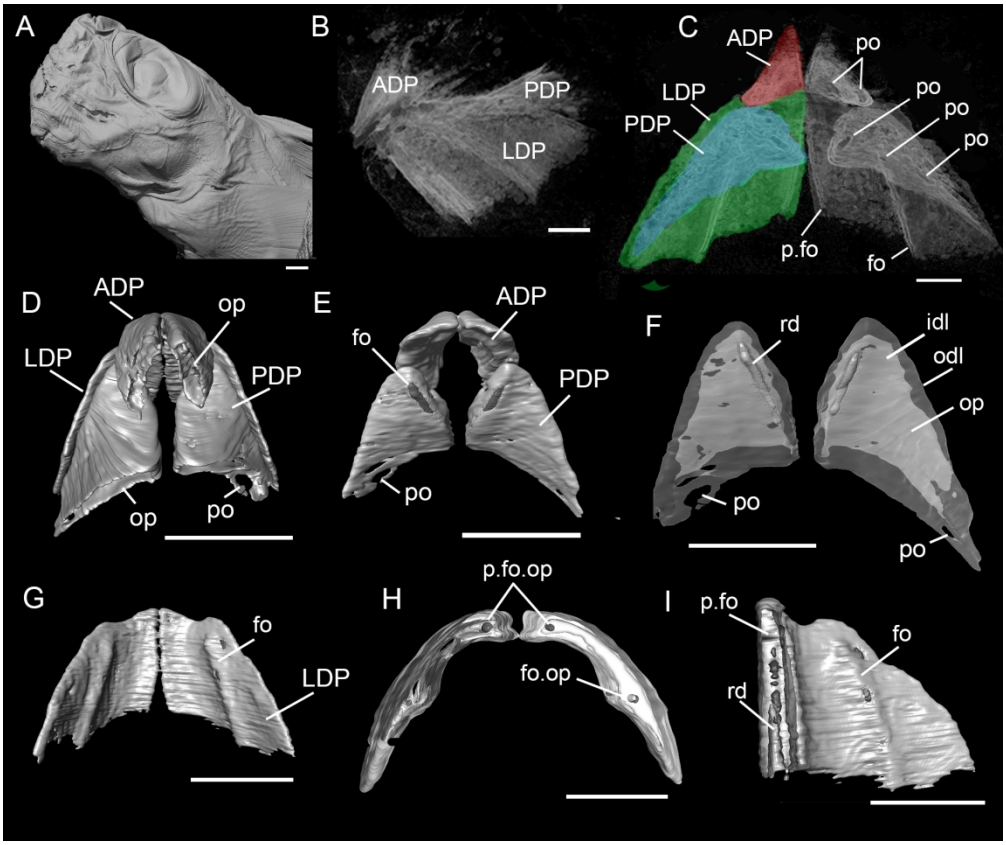


Figure 4 Family Chimaeridae, Hydrolagus affinis. (A–I), BMNH2003.11.16, small juvenile, UK. (A) lateral view of head; (B) labial view of upper and lower dental plates in association (softer tissues including jaw cartilage removed virtually); (C) dorsal (visceral) view of upper and lower dental plates, in association with, and overlying, the lower dental plates. On left side of the image, false colour red indicates the anterior upper dental plate and blue the posterior upper dental plate. Green represents the lower dental plate. On the right side of the image, openings (pores) are visible on the margins of the upper dental plates, and folds on the lower plate (compare to Fig. 2); (D) dental plates in occlusion, upper plates in visceral view, oral margin of lower dental plates visible, with different segmentation parameters compared to (C). Open margins visible on the anterior and posterior dental plates. (E) upper dental plates in oral view, showing parasymphysial folds and more posterior pores; (F) modified segmentation settings showing outer dentine layer (dark grey) and inner cavity (light) grey; G) lower dental plates in oral view; (H) virtual transverse section through lower plates, showing openings in folds on the oral surface; I) virtual section through fold, showing dentine rod within. Abbreviations as in previous plates, also: fo.op, opening in dental plate fold; idl, inner dentine layer; odl, outer dentine layer; op, open margin of dental plate; p.fo.op, opening in parasymphysial dental plate fold. Scale bar A–C= 1 cm; D=5mm; E= 3mm; F–I= 2.5mm.

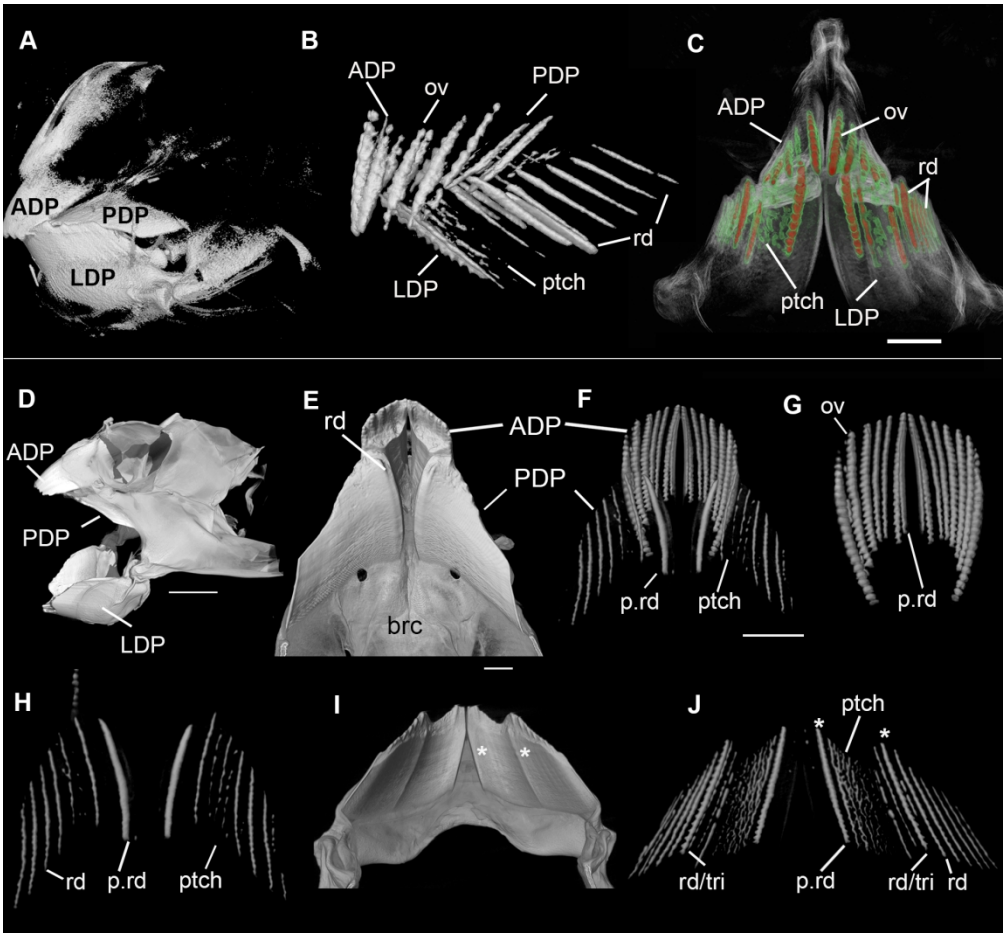


Figure 5 Family Chimaeridae, Hydrolagus affinis. (A–C), small juvenile, Scotland. (A, B) upper and lower dental plates in association, lateral view, (B) with surrounding tissues removed virtually to show mineralized rods, ovoids and patches; (C) upper and lower dental plates in association, anterior view, false coloured to show mineralized elements (red) and surrounding dentine (green). (D–J), larger juvenile, Scotland. (D), skull and lower jaw, lower jaw and upper and lower dental plates in lateral view; (E–H) upper dental plates in oral view, (F–H) plates virtually dissected to show mineralized rods, ovoids and patches; (I, J) lower dental plate, oral view; (J) surrounding dentine removed virtually to show mineralized dentine forming rods and patches, asterisks indicate position of elongate rods associated with folds on the dental plate surface. Abbreviations as in previous plates, also ptch, patch of irregular mineralization; rd/tri, rod that will develop into tritor in later growth stages. Scale bar= 0.5 cm.

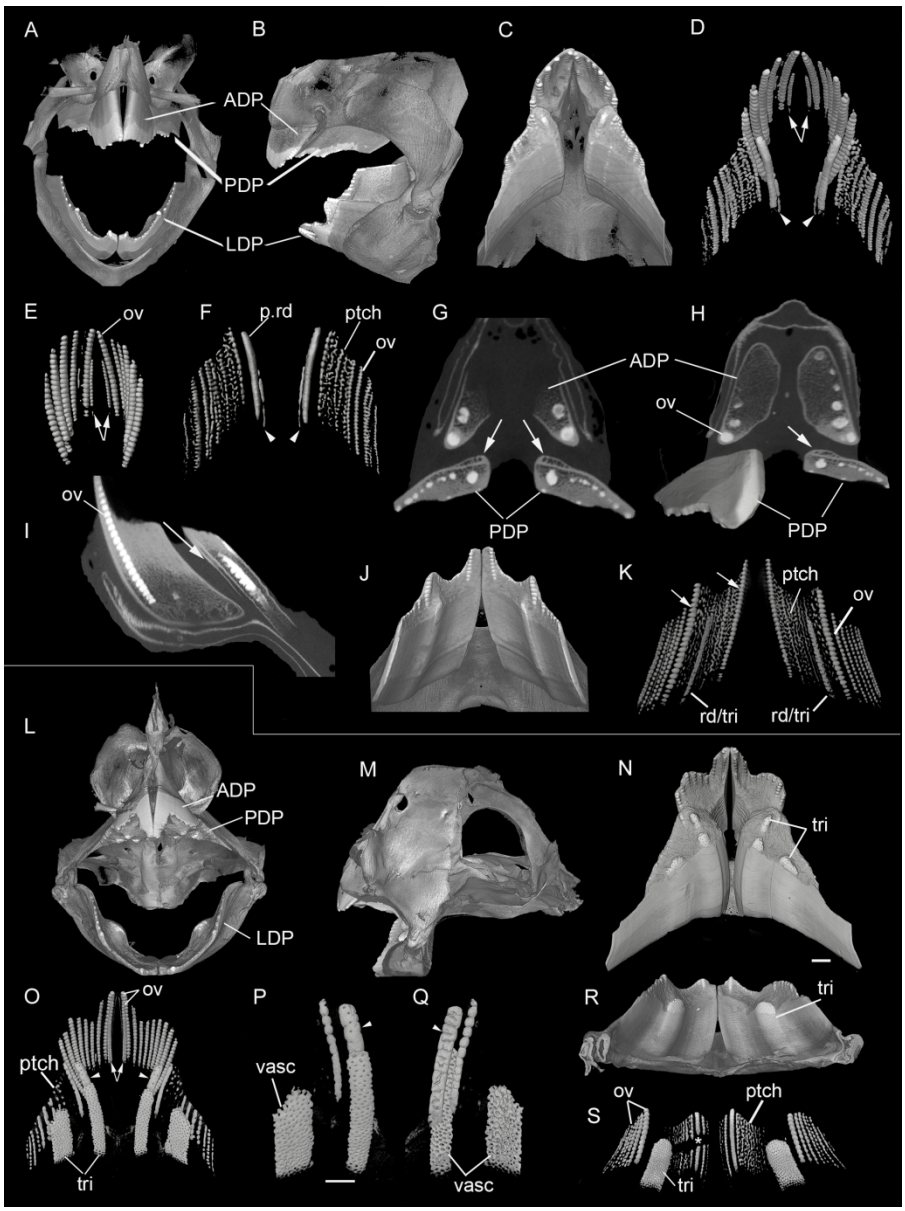


Figure 6 Family Chimaeridae (A–K) Hydrolagus pallidus, large adult, Scotland. (A, B) jaws and dental plates in (A) anterior; (B) lateral views. (C–I) upper anterior and posterior dental plates, in oral view; (D–F) surrounding tissue virtually removed to show rods, ovoids, patches for (E) anterior, (F) posterior plates, arrows and arrowheads indicate newly developing rods. (G–I) virtual sections through upper dental plates to show developing ovoids (G, H, transverse section; I, longitudinal section), white arrows indicate aboral territory (compare to Fig. 1). (J, K) lower dental plate in (J) oral view; (K) surrounding tissue virtually removed to show rods, ovoids and patches. (L–S) Chimaeridae indet, skull of probable adult, commercial supplier, probably Philippines. Skull, jaws and dental plates in (L) anterior; (M) lateral views; (N–Q) upper anterior and posterior dental plates in oral view; (O–Q) surrounding tissue virtually removed for anterior and posterior plates, arrows indicate new parasymphysial element added, arrowheads showing position of developing tritor in the posterior dental plate; (P, Q) hypermineralized tissue in (P) oral and Q) visceral views, arrowheads show position of developing tritor including grooves marking the visceral surface. (R, S) lower dental plate in (R) oral view; (S) with surrounding tissue virtually removed. Abbreviations as in previous Figures. Scale bar=1.5cm

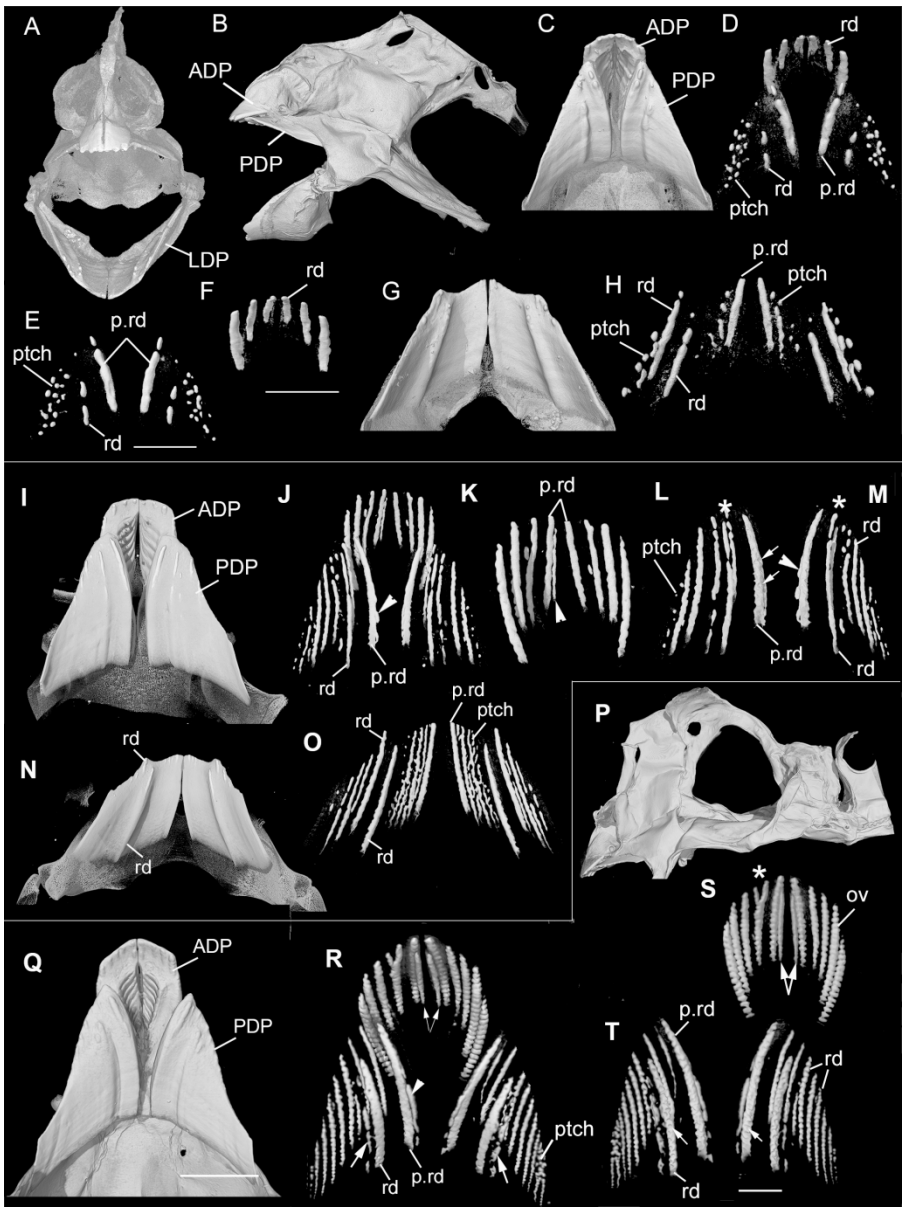


Figure 7 Chimaera monstrosa (A–H) Chimaera monstrosa juvenile, Scotland. Skull, jaws and dental plates in (A) anterior; (B) lateral views (anterior to left). (C–F) upper anterior and posterior dental plates in oral view; (D–F) surrounding tissue virtually removed for anterior and posterior plates to expose rods and patches, including in the (E) posterior and (F) anterior dental plates. G, H) lower dental plate in G) oral view; H) surrounding tissue virtually removed. (I–O) Chimaera monstrosa juvenile, Scotland, upper and lower dental plates; (I–M) upper plates in oral view; (J–M) surrounding tissue virtually removed for anterior and posterior plates; (L, M) hypermineralized dentine in the posterior dental plate shown in (L) oral and (M) visceral views. Arrowheads indicate new dentine being added to the parasymphysial rod (J, M), new parasymphysial rod forming (K); arrows indicate grooves and circular openings developing on the surface of the rod (L); asterisks indicate second smaller, more anterior rod forming (L, M); (N, O) lower dental plate in (N) oral view; (O) surrounding tissue virtually removed. (P–T) Chimaera monstrosa, immature male (very small claspers), Scotland. Skull and upper dental plates in (P) lateral view (anterior to left). (Q–T) upper anterior and posterior dental plates in (Q) oral view; (R) surrounding tissue virtually removed for anterior and posterior plates and for (S) anterior and (T) posterior plates. Arrowheads indicate new dentine being

added to the parasymphysial rod (R), paired arrows mark new parasymphysial rod forming (R, S); single arrows indicate grooves and circular openings developing on the surface of the rod (T). Abbreviations as in other Figures. Scale bar = 5 mm.

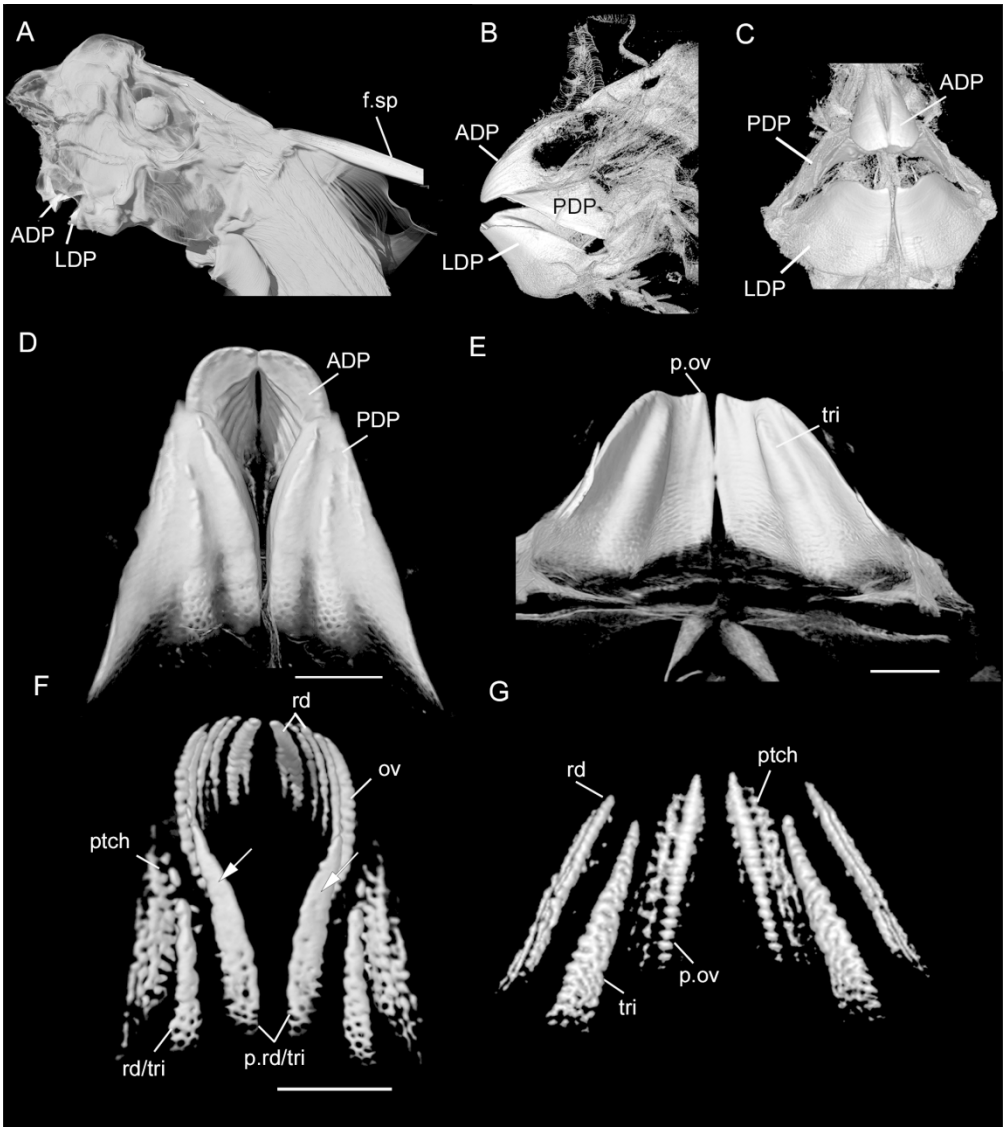


Figure 8 Chimaera sp. (A–G) Chimaera sp. indet., juvenile, commercial supplier, Taiwan. (A) skull, jaws, dental plates, part of the body including dorsal fin and spine in lateral view; (B, C) associated dental plates in (B) lateral and (C) anterior views. (D, F), upper anterior and posterior dental plates in oral view; (F) surrounding tissue virtually removed from both plates; (E, G) lower dental plate, (G) surrounding tissue virtually removed. Arrows (F) indicate anterior part of tritoral pad lacking opening for vascular canals. Scale bars= 4mm (D, F); 3mm (E).

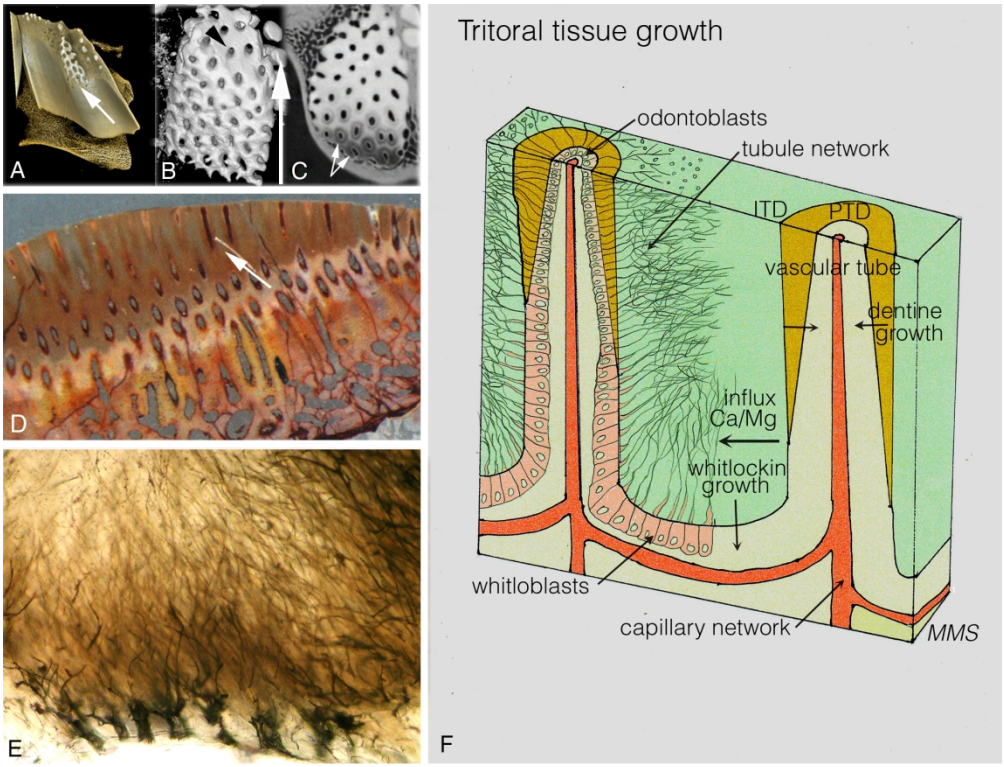


Figure 9 (A-C), Harriotta raleighana; tritoral hypermineralized dentine formation, to illuminate tissue structure of the plate morphology, in (A) lower jaw of a younger individual, CT-scan 3D rendered of tritoral tubate dentine surface (arrow; from Smith et al. 2019: fig. 16B). (B, C) adult upper jaw tritoral pad, (B) CT-scans 3D density rendered, from mature whitlockin at the oral, exposed surface, to forming whitlockin more basally (arrow); (C) a horizontal virtual section of the same region with many regular vascular tubes on the exposed surface, in the forming tissue these have rings of less dense peritubate dentine (white arrows; Smith et al., 2019: fig. 17). (D) Strebelodus oblongus (NHMUK PV P75426), sectioned dental plate shows fossil histology vertical to the punctate surface from oral to visceral, of tubate dentine in a tritor (arrow indicating two tubes), showing three zones of development of continuous mineralization, with parallel vascular tubes, normal to the oral surface, emanating from the larger vascular spaces in the trabecular dentine. (E) Harriotta raleighana (from Smith et al., 2019: fig. 6E), section of mineralized tissue of a tritoral pad, same plane as in (D) at high resolution, of cell spaces at the forming front, linked with a complex mass of increasingly fine diameter tubules emanating from the cell spaces in the first formed whitlockin, nearby many vascular capillaries (not shown but are represented in (F). (F) schematic, interpretive diagram of living tissue with cells responsible for whitlockin formation of a tritor as in (E), around two of the vascular tubes (e.g., arrow in D), comparable to those that make up all of this tissue (see surface views A–C). Images in Figure 9A, E reproduced under Creative Commons attribution license, BMC (Smith et al. 2019: https://doi.org/10.1186/s40851-019-0125-3)

| Specimen/Taxon | Figure | Voxel size (µm) | kV | µA | filters (mm) | Number of projections |
|---|---|---|---|---|---|---|
| *Callorhinchus milii*, embryo or neonate, Western Port bay, Victoria, Australia | 2A-G | 26 µm | 204 | 184 | Cu 0.250 | 3142 |
| *Callorhinchus milii*, early growth stage Western Port bay, Victoria, Australia | 2H-L | ----- | ----- | ----- | ----- | ----- |
| *Callorhinchus milii*, adult, uncatalogued NHM Palaeo specimen (Patterson, 1965) | 2M-O | 8.1156 µm | 120 | 84 | None | 3201 |
| *Callorhinchus callorhynchus*. Uruguay, smaller adult | 3A-G | ----- | ----- | ----- | ----- | ----- |
| *Callorhinchus callorhynchus*. Uruguay, smaller adult | 3H-M | 0.028613; 28µm | 195 | 190 | Cu 0.250 | 3142 |
| *Hydrolagus affinis* BMNH2003.11.16, small juvenile, UK | 4A-I | 31µm | 130 | 190 | None | 3142 |
| *Hydrolagus affinis* small juvenile, Scotland | 5A-C | 31µm | 130 | 190 | None | 3142 |
| *Hydrolagus affinis* larger juvenile, Scotland | 5D-I | 48µm | 190 | 160 | Cu 0.250 | 3142 |
| *Hydrolagus pallidus*, large adult, Scotland | 6A-K | 30µm | 200 | 180 | Cu 0.100 | 3142 |
| Chimaeridae indet, skull of probable adult, Phillippines | 6L-S | 40µm | 200 | 160 | Cu 0.250 | 3142 |
| *Chimaera montrosa* juvenile, Scotland | 7A-H | 41µm | 175 | 165 | Cu 0.100 | 3142 |
| *Chimaera montrosa* juvenile, Scotland | 7I-O | 3-6 µm | 70 | 114 | Al | ----- |
| *Chimaera monstrosa*, immature male Scotland | 7P-T | 32µm | 165 | 170 | Cu 0.100 | 3142 |
| Chimaera sp. indet., juvenile, Taiwan. | 8 | 39µm | 179 | 165 | Cu 0.100 | 3142 |
| | | | | | | |

**Table 1:** list of x-CT parameters.

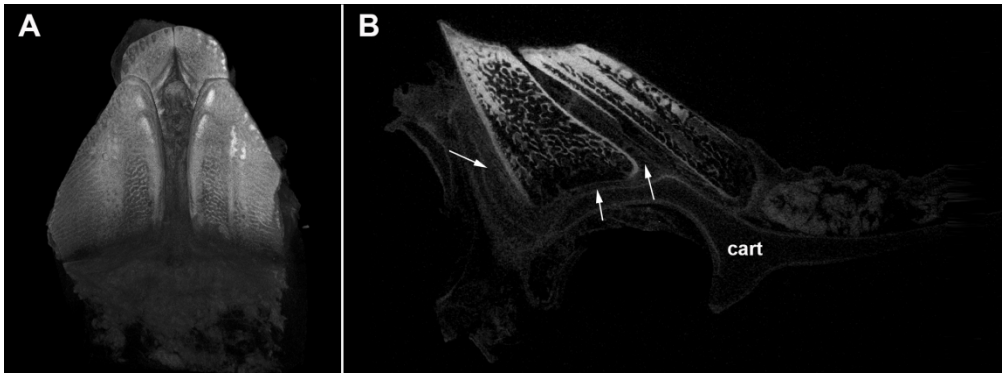


182x67mm (300 x 300 DPI)